DOCUMENTOS DE TRABAJO

Conditional Bayesian Quantile Regressions for Forecasting the GDP Growth Distribution in a Small Open Economy

Jorge Fornero
Carlos Molina

N° 1081 Mayo 2026
BANCO CENTRAL DE CHILE

banco central Chile

Documentos de Trabajo del Banco Central de Chile
Working Papers of the Central Bank of Chile
Agustinas 1180, Santiago, Chile
Teléfono: (56-2) 3882475; Fax: (56-2) 38822311

Documento de Trabajo N° 1081

Working Paper N° 1081

Conditional Bayesian Quantile Regressions for Forecasting the GDP Growth Distribution in a Small Open Economy*

Jorge Fornero
Banco Central de Chile

Carlos Molina
Banco Central de Chile

Resumen

Estimamos la distribución predictiva completa del crecimiento del PIB en una economía pequeña y abierta, usando Chile como caso de estudio. Siguiendo Sokol (2025), implementamos la regresión de cuantil bayesiana condicionando en adelantos de variables internas y en un conjunto amplio de información resumida en factores externos y domésticos. Encontramos que las condiciones del mercado laboral y financieras mejoran sustancialmente la precisión predictiva fuera de la muestra, reducen las puntuaciones de pérdida de cuantiles y permiten la identificación temprana de riesgos de cola y episodios de contracción en comparación con los modelos basados únicamente en información contemporánea del crecimiento del PIB. Además, el marco facilita la construcción de gráficos de abanico condicionales que capturan asimetrías consistentes con proyecciones de la tasa de desempleo.

Abstract

We estimate the full predictive distribution of GDP growth in a small open economy, using Chile as a case study. Following Sokol (2025), we implement a Bayesian conditional quantile regression framework that conditions on leads of domestic variables and on a broad information set summarized by foreign and domestic factors. Our results show that domestic labor-market and financial conditions substantially improve out-of-sample predictive accuracy, reduce quantile loss scores, and allow earlier identification of tail risks and contraction episodes relative to models relying solely on contemporaneous information of GDP growth. In addition, the framework enables the construction of conditional fan charts that exhibit asymmetries consistent with projected unemployment dynamics.

* We thank Andrej Sokol for generously sharing his code, and Andrés Sagner for providing his dataset. We are also grateful to Markus Kirchner, Benjamin García, Luigi Durand, Andrés Ghini, and our colleagues for their valuable comments and insights. We further thank an anonymous referee at the Central Bank of Chile. Finally, we thank Andrés Gallardo and Ignacio Leiva for excellent research assistance. The views and conclusions in this paper are those of the authors and do not necessarily reflect the position of the Central Bank of Chile or its Board members.
E-mail addresses: jfornero@bcentral.cl; cmolina@bcentral.cl.

1 Introduction

Macroeconomic forecasting has traditionally focused on estimating the conditional mean of key variables, such as GDP growth, while comparatively less attention has been devoted to the variance and other moments of the predictive distribution. Many central banks illustrate the uncertainty surrounding projections using fan charts, typically constructed under the assumption of normally distributed forecast errors.[1]

The experience of major shocks, including the Global Financial Crisis (GFC) and the Covid-19 Pandemic, has underscored the limitations of mean-centric forecasts and highlighted the importance of systematically assessing the risks surrounding baseline projections. Consequently, examining the complete predictive distribution over the forecast horizon has become increasingly valuable for policymakers, both to quantify the likelihood of adverse outcomes (such as negative growth) and to communicate alternative scenarios in a more transparent and informative manner.

A widely used approach to estimate complete distributions is the *at-risk* framework proposed by Adrian et al. (2019). This method relies on a two-step procedure to estimate the distribution of GDP growth conditional on economic and financial conditions. In the first step, the relationship between GDP growth percentiles and predictors is estimated using quantile regressions (Koenker and Basset, 1978). In the second step, conditional quantiles are fitted to a flexible parametric distribution, the skewed-t distribution of Azzalini and Capitanio (2003), which allows for fully specified conditional densities of GDP growth at each point in time and enables the evaluation of its various moments.

Moreover, the empirical literature applying the *at-risk* approach has primarily focused on modeling the distribution of GDP conditional on financial indicators (Adrian et al., 2019; Alvarez et al., 2021; Ossandon et al., 2022), while variables such as global activity, international inflation, or commodity prices have re-

[1] For example, since 1997, the Bank of England's Monetary Policy Reports have included fan charts for inflation. Britton et al. (1998) presents a methodology for constructing flexible fan charts based on the two-piece normal (2PN) distribution, characterized by three parameters: the mode (m), the standard deviation (σ)—often proxied by historical forecast errors—and an asymmetry parameter (γ) that captures cases where probability mass shifts toward the upside or downside. Fornero and Gatty (2020) conducts a back-testing exercise of fan charts published in Chile's Monetary Policy Reports.

ceived considerably less attention. This is notable given a growing body of evidence—including Mumtaz and Surico (2009), Charnavoki and Dolado (2014), Bjørnland et al. (2017), and Lyu et al. (2021)—showing that international factors can play a significant role in shaping GDP dynamics in small open economies. This gap motivates a systematic examination of how external variables contribute to density forecasts within the *at-risk* framework.

A recent contribution by Sokol (2025) addresses part of this challenge by introducing a conditional quantile regression approach that incorporates expert judgment and technical assumptions into a standard Bayesian quantile regression framework (Yu and Moyeed, 2001; Kozumi and Kobayashi, 2011; Khare and Hobert, 2012). The resulting model—referred to as Conditional Quantile Regression (CQR)—extends conventional quantile regression methods to the direct multistep forecast (DMS) framework of McCracken and McGillicuddy (2019), who compare the predictive performance of iterated versus direct projection strategies. Because these methodological developments are relatively recent, most empirical applications still abstract from future conditional information when generating forecasts or assessing risks.

The objective of this paper is to evaluate the predictive contribution of external and domestic factors to GDP growth at different points of the predictive distribution, and to assess how conditioning on future trajectories of key variables—particularly the unemployment rate—affects GDP-growth density forecasts. The performance of the methodology is examined through empirical exercises using Chile as a case study.

To this end, we extend the *at-risk* framework of Adrian et al. (2019) along two dimensions. First, we incorporate global factors—such as economic activity, inflation, and commodity prices—rather than restricting attention to domestic financial conditions. Second, we implement the Bayesian conditional approach of Sokol (2025), which delivers predictive densities consistent with the future evolution of conditioning variables. This conditioning can be operationalized through technical assumptions—for example, using leads of the unemployment rate—that shift the predictive distribution of GDP growth and improve anticipation of

tail events.[2] This approach also offers greater efficiency and flexibility relative to its frequentist counterpart, as it integrates prior information and employs shrinkage techniques to mitigate the impact of a large set of regressors on parameter uncertainty.

This paper is closely related to Alvarez et al. (2021), who studies how a local financial conditions index shapes the predictive density of GDP. It differs in three main ways. First, we evaluate the predictive performance of the *at-risk* framework using a pseudo-out-of-sample exercise, rather than focusing solely on in-sample measures. Second, we employ a more flexible and efficient Bayesian framework that incorporates both lags and leads of the regressors. Third, we extend the analysis to include both external and domestic factors, rather than limiting attention to domestic financial conditions.

Regarding the main results, the out-of-sample forecasting exercises show that the proposed methodology substantially improves the ability to anticipate the future distribution of GDP growth. Models that combine domestic financial factors with labor market information, including leads of the unemployment rate, deliver the lowest quantile loss scores and the largest gains across all regions of the distribution, capturing tail risks more accurately than the benchmark model based solely on contemporaneous GDP growth. In contrast, specifications that include only global factors or financial indicators provide marginal predictive value. Taken together, these results indicate that the interaction between financial and labor market conditions is critical for explaining growth in small open economies such as Chile, whereas global factors add little additional predictive power.

The empirical applications illustrate the potential of the methodology for risk monitoring and scenario communication. Conditional densities show that models incorporating leads of observed variables assign higher probability to observed outcomes during episodes such as the GFC and the Covid-19 Pandemic, allowing extreme vulnerabilities to be detected earlier. Consistently, the 5^{th} percentile of GDP growth (Growth-at-

[2] Among the alternatives considered for technical assumptions, unemployment paths induce particularly pronounced changes in the GDP-growth distribution—an expected outcome given the relationship between GDP and unemployment formalized by Okun's law.

Risk) and the probabilities of contraction react promptly to adverse shocks, providing signals that traditional approaches fail to capture. Finally, the construction of conditional fan charts enables a more realistic representation of the balance of risks by incorporating asymmetries and scenarios consistent with projected macroeconomic conditions, overcoming the limitations of methods based exclusively on historical forecast errors. Taken together, these results consolidate the usefulness of the proposed approach as an effective tool for managing and communicating macroeconomic risks.

The remainder of the paper is organized as follows. Section 2 describes the data sources used, Section 3 details the construction of global and domestic factors through principal component analysis, Section 4 presents the methodology of conditional Bayesian quantile regressions and the estimation strategy, Section 5 reports the results of the out-of-sample forecasting exercise, Section 6 illustrates practical applications of the methodology, including conditional densities, tail risk measures (Growth-at-Risk), probabilities of GDP contraction, and conditional fan charts, Section 7 presents robustness checks, and Section 8 concludes.

2 Data

To assess the influence of external and domestic forces on the distribution of GDP, global and domestic factors are estimated from two datasets.

For the external block, we follow the methodology of Charnavoki and Dolado (2014), who identify three global factors relevant for small commodity-exporting economies. These factors are extracted from a set of international macroeconomic variables that includes indicators of global economic activity, global inflation, and international commodity prices, covering the period 1976Q1–2022Q3.[3]

Regarding domestic financial factors, the dataset used by Alvarez et al. (2021) is extended through 2022Q3. This block includes local variables associated with the stock market, credit and corporate spreads, long-term

[3]When extending the database used by Charnavoki and Dolado (2014), it was observed that the series on global exports and imports were discontinued.

bond yields, credit indicators, the real exchange rate, and terms of trade. In addition, the unemployment rate is incorporated as an observed variable.[4]

Since GDP annual growth data are available only from 1997Q1 onward, the final sample spans 1997–2022Q3. Tables B1 and B2 in the appendix provide details on the variables in each block and their sources.

3 Global and Domestic Factors

We employ principal component analysis (PCA), a standard approach that condenses information from large sets of correlated variables into a small number of orthogonal components or factors, thereby promoting parsimony and reducing multicollinearity. To ensure a unified treatment of both data blocks, we apply the same PCA framework to international and domestic indicators.

For the global factors, following Charnavoki and Dolado (2014), we apply PCA to a broad panel of international indicators—including output, industrial production, trade variables, price indices, GDP deflators, and commodity prices—to capture common external shocks without imposing structural restrictions. The specification is:

$$X_t^* = \Lambda^* F_t^* + \epsilon_t^*, \tag{1}$$

where X_t^* denotes global data, F_t^* the estimated factors, Λ^* the loading matrix, and ϵ_t^* a normally distributed error term with diagonal variance–covariance matrix R. We retain the first three principal components, which together explain approximately 82% of total variance (44%, 27%, and 11%).

We apply the same PCA procedure to the following list of domestic variables: credit spreads, stock market performance, bond yields, credit aggregates, the exchange rate, and the terms of trade.[5] This captures

[4] In additional exercises not reported for brevity, the nominal and real monetary policy rates (discounting headline CPI inflation) were included. However, no significant improvements were observed compared to the model that considers only domestic financial factors. A possible explanation is that the effects of monetary policy on GDP are transmitted through channels such as interest rates, credit costs, asset prices, and the exchange rate, which are already represented in the set of variables characterizing the local financial market.

[5] As stated in the previous section, we expand the database of Alvarez et al. (2021).

systemic financial dynamics rather than idiosyncratic noise:

$$X_t = \Lambda F_t + \epsilon_t, \tag{2}$$

where variables without asterisks denote domestic data, with factors, loadings, and idiosyncratic errors defined analogously, and an error variance–covariance matrix Q that is diagonal. We retain two components, explaining roughly 50% of variance (33% and 16%). Components explaining under 10% of variance are dropped. Results remain robust when global factors are orthogonalized to domestic ones.[6]

3.1 Estimated Factors

Figure 1 displays the factor loadings from equations (1) and (2). In the external block (left panel), the first factor (blue) loads positively on all variables, with the highest weight on global inflation. The second factor (green) is mainly associated with global activity indicators, while the third (yellow) relates primarily to commodity prices and the global commodity market activity index of Kilian (2009, 2019).

In the domestic block (right panel), the first factor (blue) loads positively on spreads, sovereign risk, financial volatility, long-term rates, and exchange-rate depreciation, and negatively on activity and terms of trade—characterizing a financial-stress component. The second factor (green) loads positively on economic activity, the stock market, and several relative prices, with mixed signs across financial variables, reflecting a business-cycle component in which activity improves alongside heterogeneous financial conditions. This co-movement aligns with the evidence in Miranda-Agrippino and Rey (2020).

[6]For comparison, see Appendix C.

Figure 1: Estimated factor loadings

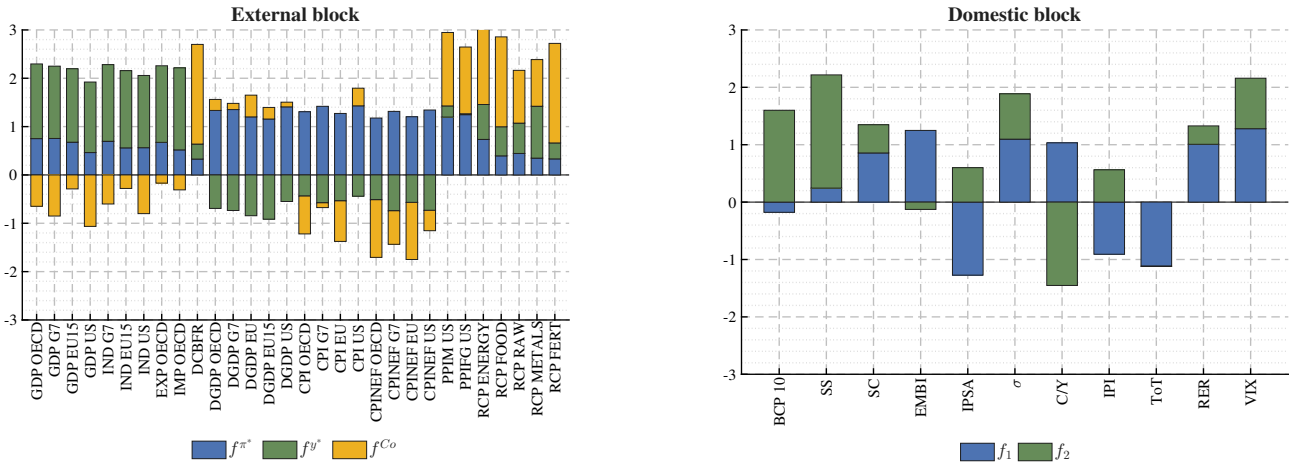

Notes: The figure shows estimated loadings for external (left) and domestic (right) factors from the factor model. Each bar represents the loading of a variable on each factor. For details on the variable definitions, see Appendix B.

Figure 2 shows the time evolution of global and domestic factors, which compactly represent the cycles affecting Chile's economy. The first global factor, associated with global activity, tracks major downturns—including the early-1980s recession, the 1991 slowdown, the 2008–09 GFC, and the sharp contraction in 2020. The second factor reflects global inflation dynamics: high inflation in the late 1970s–early 1980s, its subsequent decline, the pre-crisis rise, the post-crisis moderation, and the surge in 2021–22 driven by supply bottlenecks and energy shocks. The third factor captures commodity-price cycles, such as the late-1970s boom, the decline following the Asian crisis, the 2003–08 surge, the 2008–09 correction, and the rebound after the pandemic. These patterns are consistent with established evidence on global cycles (Kose et al., 2003; Mumtaz and Surico, 2009) and commodity-market shocks (Kilian, 2006; Hamilton, 2011).

In the domestic block, the first factor reflects financial stress episodes, with spikes during the Asian crisis, the GFC, and the Covid-19 Pandemic, consistent with Alvarez et al. (2021). The second factor is more closely tied to the business cycle: rising between 2003 and 2007 during strong expansion, falling sharply in 2008–09, recovering moderately thereafter, and rebounding around the pandemic. This suggests co-movement between activity and financial conditions without a single dominant mechanism.

Figure 2: Estimated Factors

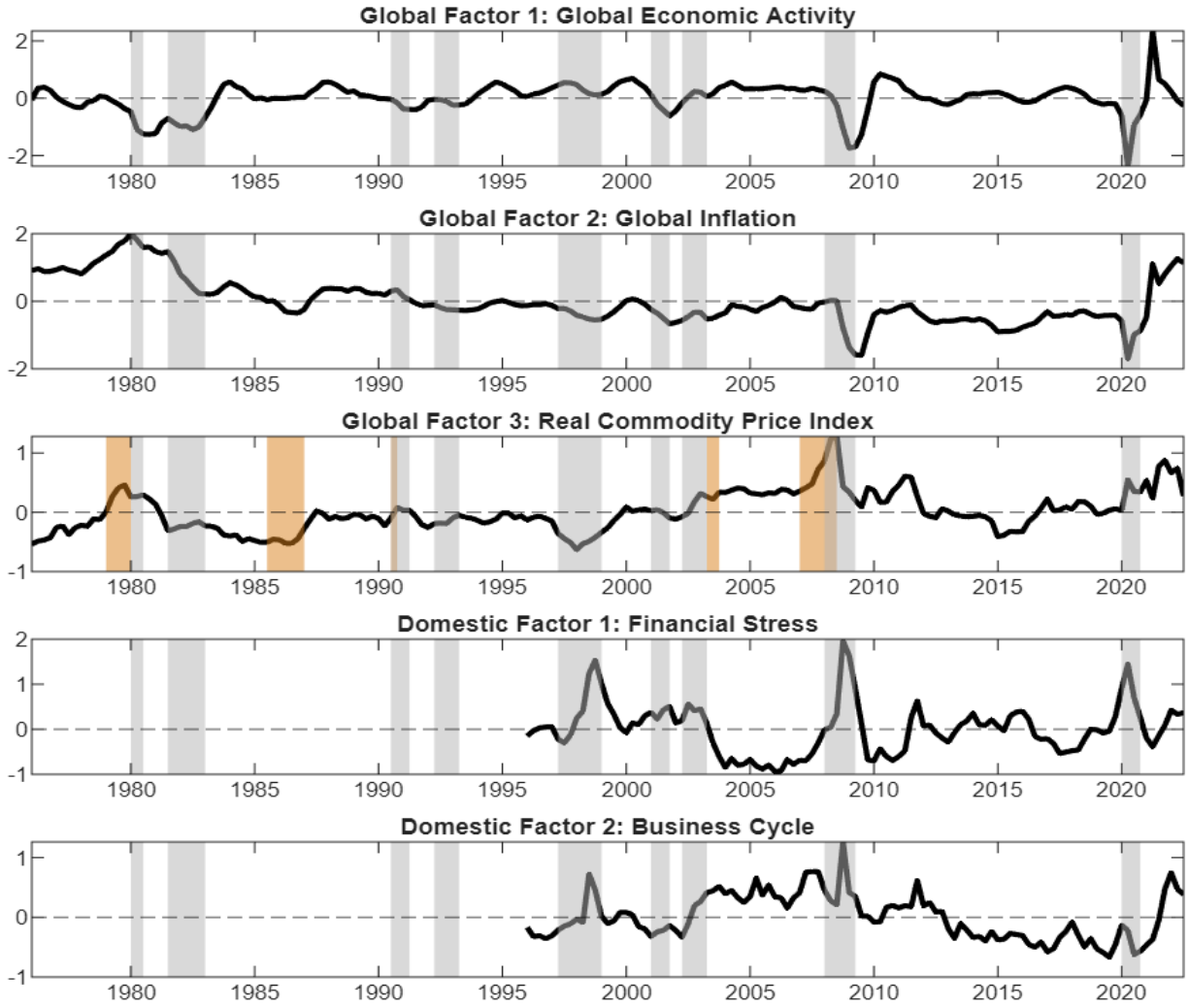

Notes: Gray (orange) shaded regions indicate major global recessions (key events in global commodity markets).

4 Methodology

To analyze the conditional distribution of future GDP growth, we adopt the Bayesian quantile regression framework of Sokol (2025), which extends the multi-step direct conditional forecasting approach of McCracken and McGillicuddy (2019). The method augments the model with projections or technical assumptions about key drivers, alongside contemporary and lagged information, and generates forecast distributions consistent with those projected paths. This enables conditional projections based not only on information

available at time t but also on anticipated trajectories of relevant variables. For each forecast horizon h, the model is specified as:

$$y_t = \alpha + \sum_{j=0}^{p-1} \beta_j' x_{t-h-j}^b + \sum_{1 \le i \le h} \gamma_i' x_{t-h+i}^f + \varepsilon_t \tag{3}$$

where the superscripts b and f denote, respectively, *backward*-looking variables (observed at or before the forecast origin) and *forward*-looking variables (technical assumptions or projections over the forecast horizon), α is a constant term, β_j coefficients multiply variables known at $t-h-j$, while γ_i coefficients multiply future values of technical assumptions. Following McCracken and McGillicuddy (2019) and Sokol (2025), coefficients are estimated using realized future values, as historical projection vintages are not consistently available. Using realized data captures the conditional relationship between y_t and actual future realizations, whereas using historical assumptions reflects the properties of the forecasting process.[7]

The conditional forecast h periods ahead is:

$$\hat{y}_{t+h} = \hat{\alpha} + \sum_{j=0}^{p-1} \hat{\beta}_j' x_{t-j}^b + \sum_{i=1}^{h} \hat{\gamma}_i' \hat{x}_{t+i|t}^f, \tag{4}$$

where $\hat{x}_{t+i|t}^f$ denotes the projected path of technical assumptions at time t.

4.1 Estimation Strategy

Equations (3) and (4) are estimated using Bayesian quantile regression under an asymmetric Laplace error distribution (Appendix A). Coefficients depend on both the forecast horizon (h) and the quantile (q). Quantile estimates are then fitted to a continuous distribution following Adrian et al. (2019), using the skewed-t specification of Azzalini and Capitanio (2003). This approach delivers full predictive densities, enabling tail-risk analysis, probabilities of contraction, and conditional fan charts.

It is important to note that the number of regressors grows rapidly with the forecast horizon and the number

[7] As noted by Sokol (2025), the latter may embed characteristics of the assumption-setting process, while the former attributes forecast errors mainly to discrepancies between assumed and realized paths.

of conditioning variables, which makes Bayesian estimation particularly suitable in this context. Shrinkage priors help control parameter uncertainty, enhancing efficiency and stability.

4.2 Methodology illustration

Figure 3 shows the conditional density of one-year-ahead GDP growth, estimated using our methodology and conditioned on GDP growth and the domestic financial factor f_1 at time t. The distribution shifts left and widens during recessions—such as the Asian crisis, GFC, and Covid-19—while concentrating on positive values and narrowing in expansions, reflecting lower uncertainty. This greater asymmetry and higher variance in stress periods align with Adrian et al. (2019) and Alvarez et al. (2021), who find that adverse financial conditions amplify tail risks.

Figure 4 tracks skewed-t parameters. In crises, location (μ) falls (lower expected growth), scale (σ) rises (greater uncertainty), skewness (α) turns negative (left-skew, higher downside risk), and degrees of freedom (ν) drop (fatter tails, more extreme events).

Together, Figures 3 and 4 show that the methodology captures shifts in the full conditional distribution—not just mean and variance—providing a richer view of growth risks across the cycle.

Figure 3: One-year-ahead predictive distribution of real GDP growth over time

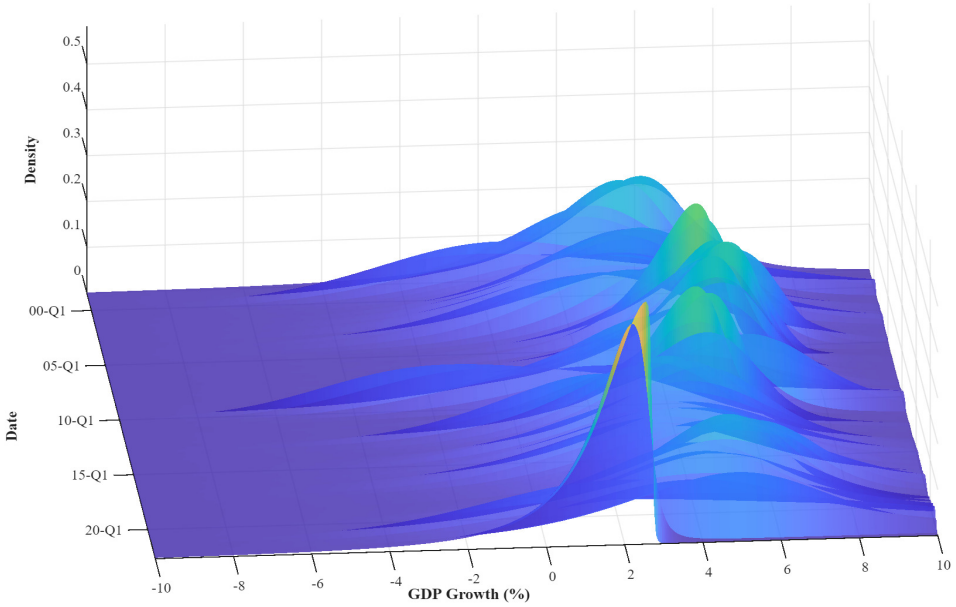

Notes: Based on quantile regressions with current real GDP growth and a domestic financial factor (f_1) as conditioning variables.

Figure 4: Evolution of skewed-t distribution parameters, one-year-ahead GDP growth $(h = 4)$

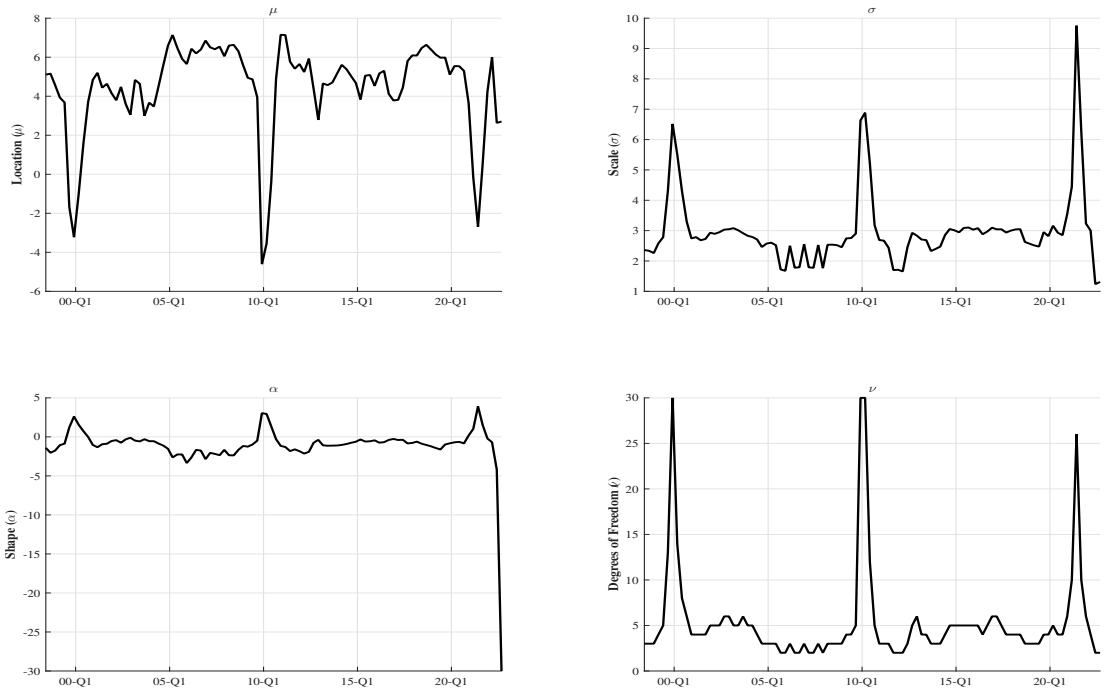

Notes: Time evolution of the four parameters (defined in the main text). Model specification described in note to Figure 3.

5 Forecast evaluation

We assess predictive performance relative to a benchmark model conditioning only on contemporaneous GDP growth. Eight alternative specifications are considered: (1) one domestic financial factor; (2) two domestic financial factors; (3) one global activity factor; (4) one global inflation factor; (5) one global commodity price factor; (6) the unemployment rate; (7) two domestic financial factors plus unemployment; and (8) the previous specification extended with unemployment leads.

A pseudo out-of-sample exercise mimics real-time data using the latest vintage, as historical vintages for financial, external factors, and unemployment are unavailable. The evaluation spans 2008Q4–2022Q3, covering 56 forecast windows against realized GDP growth up to nine quarters ahead.[8] The evaluation period begins in 2008Q4 to ensure that the initial training sample (1997Q1–2008Q4) is sufficiently large for stable Bayesian estimation, while still including two major tail episodes—the Global Financial Crisis and the Covid-19 Pandemic—within the out-of-sample window, which is essential for assessing the models' ability to capture extreme downside risks.

First, predictive performance is assessed using average quantile scores across horizons and quantiles.[9] For time t, quantile τ at horizon h, the score is:

$$QS_{t,h} = \frac{1}{N_v} \sum_{v} \rho_\tau \left(y_{t+h} - \hat{P}^{-1}_{v,h}(\tau) \right), \tag{5}$$

where N_v is the number of forecast windows and $\hat{P}^{-1}_{v,h}(\tau)$ the predicted quantile for window v.

Figure 5 reports average quantile scores by specification. The model with one domestic financial factor (f_1) performs similarly to the benchmark, while adding a second factor (f_2) improves central quantiles for

[8] The exercise produces 56 forecast origins (2008Q4–2022Q3), of which the first 47 (through 2020Q2) have realized GDP growth available at every horizon $h = 1, \ldots, 9$ and are therefore used in the scoring evaluation.

[9] Quantile scores, like other scoring rules, penalize errors more heavily in sensitive regions of the loss function, making them particularly responsive to outliers.

intermediate horizons ($h = 4, 5, 6$). Including unemployment (u_t) further enhances performance at longer horizons ($h = 7, 8, 9$).

The combination of domestic factors and unemployment ($f_1 + f_2 + u_t$) delivers systematic gains across most quantiles and horizons compared to specifications that include these elements separately and relative to the benchmark. This suggests that financial and labor conditions interact complementarily in shaping the distribution of future GDP growth. Moreover, the model incorporating future unemployment values ($f_1 + f_2 + u_t$(cond)) achieves the best performance across the entire distribution and all horizons.[10] This underscores the importance of labor market dynamics in predicting growth risks.

The role of unemployment differs markedly across specifications. When only contemporaneous unemployment is included (i.e., u_t or $f_1+f_2+u_t$), improvements are concentrated around the center of the distribution, with more limited gains in the tails. This pattern suggests that current labor market conditions are informative about the central tendency of future GDP growth, but less effective in capturing extreme downside outcomes.

By contrast, the conditional specification that incorporates leads of unemployment delivers substantial improvements across the entire distribution, particularly in the left tail. This highlights the value of conditioning GDP density forecasts on future labor-market paths when the objective is to detect downside risks and construct scenario-consistent forecast distributions. If the improvement were driven entirely by the contemporaneous Okun relationship, we would expect uniform gains across quantiles rather than the pronounced left-tail concentration observed in the conditional specification. At the same time, given the close relationship between unemployment and output at horizon $t + h$, in line with Okun's law, part of these gains may reflect the contemporaneous linkage between both variables rather than purely anticipatory content.

The heightened downside risk reflected in the left tail during recessions can be reconciled with well-documented

[10]Part of this improvement reflects counterfactual knowledge of future assumptions. Yet, the superior accuracy of real-time coefficients under these conditions reinforces the model's economic validity. Conversely, conditional forecasts that fail even with realized-data assumptions lack any claim to usefulness. Ultimately, the quality of a conditional forecast hinges on the accuracy of its technical assumptions.

labor market dynamics. In particular, job separation rates increase sharply at the onset of recessions, while quit rates decline as labor market conditions deteriorate. At the same time, job finding rates respond sluggishly and do not adjust sufficiently to offset the resulting rise in unemployment. When unemployment is used as a conditioning variable, these asymmetric and nonlinear labor market responses translate into elevated downside risks for future GDP growth. See, e.g., Kohlbrecher and Merkl (2022), Birinci and Amburgey (2021), Naudon and Pérez (2018).

It is important to note that the conditional specification relies on future realizations of explanatory variables (i.e., variables observed at horizon $t+h$), which introduces a look-ahead bias in the out-of-sample evaluation. As a result, the reported performance should be interpreted as an upper bound, since such information would not be available to policymakers in real time. Nevertheless, the exercise remains informative about the potential gains from incorporating forward-looking information into the forecasting framework.

On the other hand, global factors—economic activity, inflation, and commodity prices—do not provide significant improvements over the benchmark or relative to specifications conditioning on domestic factors.[11]

Second, predictive performance is summarized using the Gneiting and Ranjan (2011) score relative to the benchmark model, which conditions only on GDP in t:

$$GR_{t,h} = \int_0^1 QS_{t,h} w(\tau)\, d\tau, \tag{6}$$

where $w(\tau)$ is a non-negative weighting function. Intuitively, GR scores provide an aggregate measure of performance across regions of the predictive density.

[11] This conclusion reflects averages across multiple windows; however, global factors may exert greater influence on predictive distributions during specific episodes.

Figure 5: Average quantile scores

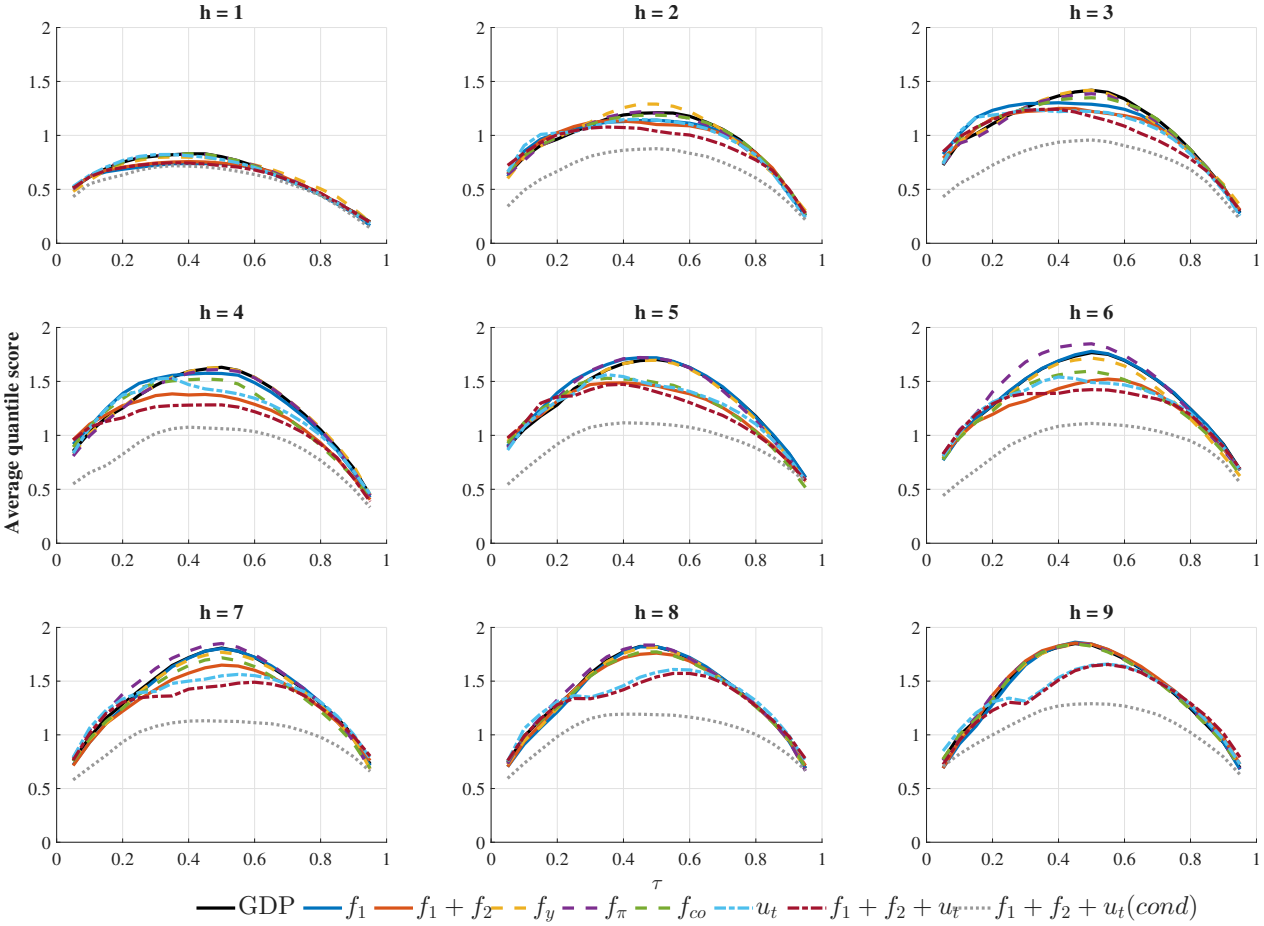

Notes: The figure reports average quantile scores (y-axis) by quantile (x-axis) for each forecast horizon h over the evaluation period 2008Q4–2022Q3 (47 vintages). Lower scores indicate better performance.

Table 1 reports GR relative scores that confirm previous findings: adding a second financial factor and unemployment (with leads) reduces scores by about 30% in both center and tails, while global factors offer no gains, with values near 1 across all regions.

Table 1: Relative Scores by Models and Horizons

Model	h=1	h=2	h=3	h=4	h=5	h=6	h=7	h=8	h=9
Unweighted									
f_1	0.94	0.99	1.00	1.02	1.02	1.00	1.00	1.00	0.99
$f_1 + f_2$	0.95	1.00	0.98	0.93	**0.95**	**0.93**	0.95	1.00	1.01
f_y	1.01	1.00	0.99	1.00	1.00	0.98	0.99	1.00	1.01
f_π	1.01	0.99	1.00	1.00	1.02	1.05	1.02	1.01	1.01
f_{co}	1.00	1.01	1.01	0.96	0.94	**0.94**	0.96	0.99	1.00
u_t	1.00	0.99	1.02	0.99	0.93	**0.94**	0.95	0.94	0.92
$f_1 + f_2 + u_t$	0.94	0.94	0.94	0.88	**0.90**	**0.89**	0.91	0.92	0.89
$f_1 + f_2 + u_t$ (cond)	0.87	**0.71**	**0.69**	**0.70**	**0.71**	**0.69**	0.74	0.78	0.78
Centre									
f_1	0.94	0.99	0.98	1.01	1.02	1.01	1.00	1.00	1.00
$f_1 + f_2$	0.94	1.00	0.96	0.90	**0.93**	**0.92**	0.95	1.00	1.01
f_y	1.01	1.01	0.98	1.00	1.00	0.98	0.99	1.00	1.01
f_π	1.01	0.98	0.99	1.00	1.02	1.06	1.02	1.01	1.01
f_{co}	1.00	1.01	1.00	0.96	**0.94**	**0.94**	0.96	0.99	1.00
u_t	1.00	0.99	1.02	0.98	0.92	**0.92**	0.94	0.92	0.90
$f_1 + f_2 + u_t$	0.93	0.92	0.92	**0.85**	**0.88**	**0.86**	**0.89**	0.90	0.86
$f_1 + f_2 + u_t$ (cond)	0.87	**0.72**	**0.69**	**0.70**	**0.71**	**0.69**	**0.72**	0.77	0.76
Tails									
f_1	0.95	0.99	1.07	1.06	1.02	1.00	0.99	0.98	0.97
$f_1 + f_2$	0.97	1.02	1.05	1.00	0.99	**0.96**	0.97	1.00	1.00
f_y	0.99	0.99	1.02	1.00	1.00	0.97	0.99	0.99	1.01
f_π	0.99	1.00	1.00	0.99	1.00	1.04	1.01	1.00	1.01
f_{co}	1.00	1.01	1.02	0.99	0.95	**0.95**	0.97	1.00	1.01
u_t	1.00	1.00	1.00	1.00	0.95	0.98	1.01	1.01	1.00
$f_1 + f_2 + u_t$	0.96	1.01	1.03	0.95	0.97	0.97	0.99	1.01	0.97
$f_1 + f_2 + u_t$ (cond)	0.85	**0.68**	0.69	**0.70**	0.73	0.69	0.78	0.82	0.84
Right Tail									
f_1	0.95	0.98	0.96	0.98	1.00	1.00	1.00	1.01	1.00
$f_1 + f_2$	0.97	0.99	0.95	0.89	**0.90**	**0.94**	0.97	1.00	1.02
f_y	1.04	1.01	1.00	1.00	0.98	0.96	0.98	1.00	1.00
f_π	1.01	0.99	1.00	1.00	1.00	1.02	1.00	1.00	1.00
f_{co}	1.00	1.01	1.00	0.93	**0.90**	**0.92**	0.95	0.99	1.00
u_t	0.99	0.98	1.01	1.00	0.93	0.94	0.98	0.98	0.96
$f_1 + f_2 + u_t$	0.96	0.91	0.89	**0.85**	**0.88**	0.90	0.95	0.97	0.96
$f_1 + f_2 + u_t$ (cond)	0.88	**0.73**	**0.72**	**0.72**	**0.75**	**0.72**	**0.75**	0.80	0.80
Left Tail									
f_1	0.94	1.00	1.06	1.06	1.03	1.00	0.98	0.98	0.98
$f_1 + f_2$	0.94	1.02	1.02	0.99	1.00	**0.94**	**0.94**	0.99	1.00
f_y	0.98	1.00	0.99	0.99	1.01	0.99	1.00	0.99	1.01
f_π	1.00	0.99	1.00	1.00	1.03	1.08	1.04	1.02	1.01
f_{co}	1.00	1.01	1.01	1.00	0.99	**0.96**	0.97	1.00	1.01
u_t	1.01	1.00	1.02	0.98	0.93	0.94	0.95	0.93	0.92
$f_1 + f_2 + u_t$	0.93	0.99	1.01	0.93	0.95	0.91	**0.90**	0.91	0.86
$f_1 + f_2 + u_t$ (cond)	0.85	0.68	**0.66**	**0.68**	0.68	0.65	0.74	0.78	0.79

Notes: The table reports relative Gneiting and Ranjan (2011) scores over the forecast evaluation period 2008Q4 to 2022Q3 (47 vintages). The weight functions are given by $w_0 = 1$ (unweighted), $w_1(\tau) = \tau(1-\tau)$ (central region), $w_2(\tau) = (2\tau - 1)^2$ (tails), $w_3(\tau) = \tau^2$ (right tail), and $w_4(\tau) = (1-\tau)^2$ (left tail). An entry < 1 indicates that the augmented model performs better than the model that conditions only in GDP in t in the region of interest. Scores for the conditional specification $f_1 + f_2 + u_t$ (cond) use realized unemployment values and should be interpreted as an upper bound on operational performance. Scores where the hypothesis of equal forecast accuracy is rejected at the 10% confidence level or higher based on the Diebold and Mariano (1995) test with the Harvey et al. (1997) finite-sample correction are highlighted in bold.

The limited predictive power of models relying exclusively on domestic financial factors, relative to the benchmark, is consistent with the findings of Plagborg-Møller et al. (2020) for advanced economies, where financial variables contribute minimally to conditional density forecasts once real variables are incorporated. Similarly, the weak role of global factors may reflect the transmission mechanisms of external shocks in small open economies such as Chile, which operate primarily through trade—via terms of trade and the real exchange rate—and through financial channels associated with credit costs and liquidity. These effects are largely embedded in the variables used to construct domestic financial factors (see Figure 1). Consequently, global shocks to activity, inflation, and commodity prices are indirectly captured through asset prices, spreads, and local interest rates, thereby reducing the incremental predictive value of external factors.

Additionally, to assess whether global factors provide additional predictive content beyond domestic financial conditions, we estimate joint specifications combining both sets of variables. The results in Table C2 of Appendix C show that the inclusion of global factors yields only limited additional gains relative to specifications with domestic financial factors alone. This suggests that the predictive information contained in global variables is largely captured by domestic financial conditions. Furthermore, to evaluate whether the role of global factors is amplified during episodes of pronounced external shocks, Table C3 reports relative scores for the pre-COVID subsample (2008Q4–2017Q3), excluding the pandemic and post-COVID commodity price shocks. The ranking of model specifications is preserved, confirming that the limited predictive contribution of global factors is not driven by the high-volatility period of 2020–2022.

This finding is consistent with a transmission mechanism in which global shocks affect the domestic economy primarily through financial channels, such as asset prices, credit conditions, and exchange rates. In this sense, domestic financial factors appear to capture most of the relevant predictive content of global conditions for GDP growth.

Third, global calibration is assessed in Figure 6 using probability integral transforms (PITs), which test

whether predicted probabilities align with observed frequencies. A well-calibrated model should approximate the 45° diagonal and remain within the confidence bands proposed by Rossi and Sekhposyan (2019). At short and medium horizons ($h = 2$–5), most specifications exhibit deviations from uniformity but remain within the bands. For horizons $h \geq 6$, PITs diverge more markedly, particularly for the specification conditioning on local factors and unemployment leads, which shifts above the diagonal, indicating overestimation in certain ranges. In contrast, the specification based solely on contemporaneous unemployment yields PITs closer to uniformity. Overall, these findings underscore a fundamental trade-off: incorporating leading indicators enhances tail-risk detection and early-warning capabilities, yet compromises global calibration.

Figure 6: Probability integral transformations

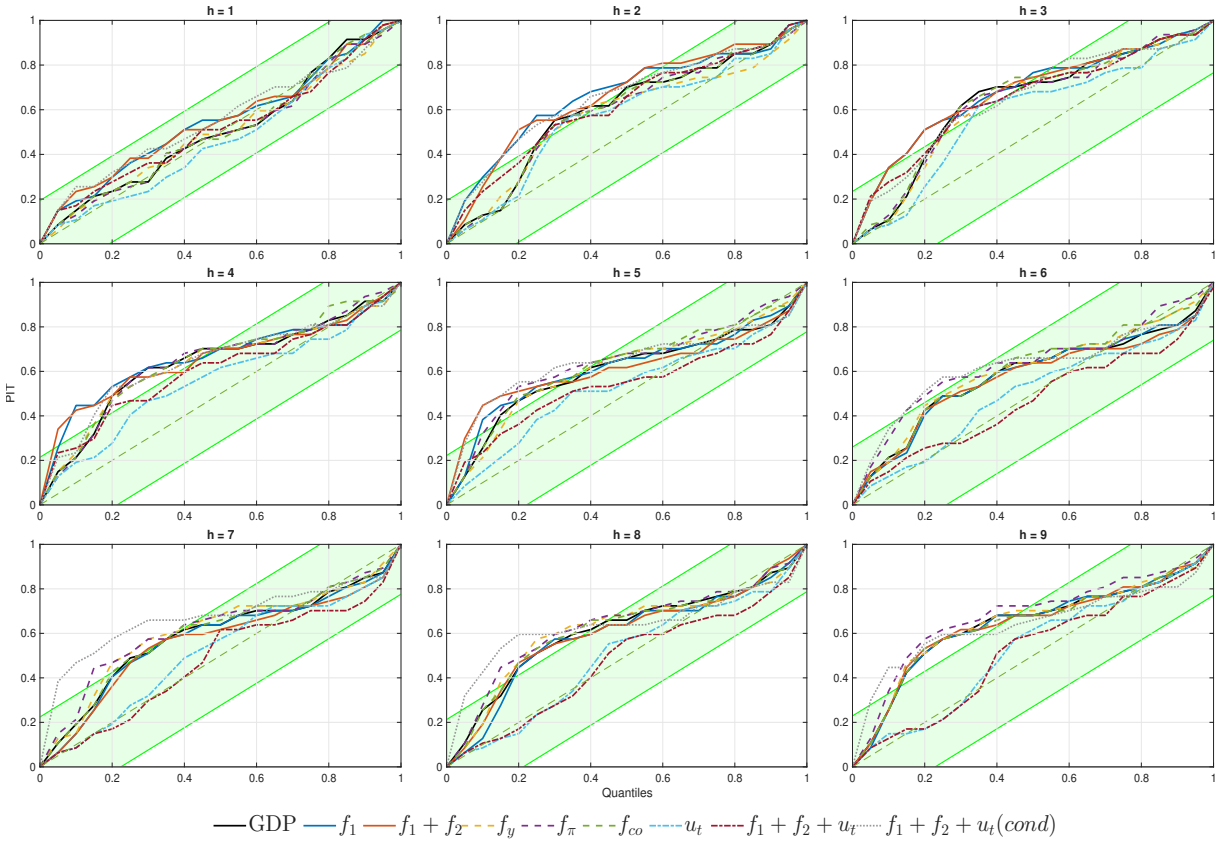

Notes: The PIT of a forecast is defined as the predictive cumulative distribution function evaluated at the data outturn. Each panel shows the empirical distributions of the models' forecast vintages, with the x-axis showing quantiles of outturns. A well-calibrated model should deliver an empirical distribution close to the diagonal. 5% critical values for the Rossi and Sekhposyan (2019) test are shown in green.

Overall, the evidence presented in this section indicates that incorporating a second domestic financial fac-

tor, together with both contemporaneous and leading unemployment rates, consistently improves predictive performance relative to the benchmark model widely used in the literature, which conditions only on GDP growth and a financial conditions index at time t (Adrian et al., 2019; Alvarez et al., 2021; Ossandon et al., 2022). However, these gains come with some deterioration in global calibration, highlighting an important trade-off for policy applications. Specifically, if the objective is the early detection of downside risks and tail events, the conditional specification dominates, as it delivers more accurate estimates of lower quantiles. By contrast, if the goal is the communication of coherent and well-calibrated predictive distributions such as in policy reports, the benchmark specification is preferable, as it provides a more reliable global representation of the predictive density.

6 Applications

This section demonstrates the application of Bayesian conditional quantile regression methodology to macro-financial risk monitoring and scenario communication. Four practical uses are considered: (i) analysis of conditional densities around crisis episodes to assess the models' ability to capture extreme vulnerabilities; (ii) estimation of the 5^{th} percentile of GDP growth as a measure of tail risk (Growth-at-Risk), useful for anticipating adverse scenarios; (iii) computation of probabilities of future negative GDP growth, enabling the transformation of continuous distributions into operational indicators for economic policy; and (iv) construction of activity fan charts for communicating macroeconomic scenarios.

6.1 Conditional Densities

Figure 7 compares in-sample conditional densities estimated by the different models around three crisis episodes: the Asian crisis, the GFC, and the Covid-19 Pandemic. At short horizons (left panel), the distributions are relatively symmetric and concentrated in positive values, indicating that most specifications did not anticipate severe contractions in activity. This is particularly evident during the pandemic, when the

observed outcome (-16.2%) lies far below the estimated densities, underscoring the difficulty of capturing extreme shocks in the very short term.

At a one-year horizon (right panel), the densities exhibit a more pronounced leftward shift and thicker tails, suggesting a higher probability of adverse outcomes. Among the specifications considered, the model conditioning on two financial factors and the unemployment rate—including leading information—assigns greater mass to the observed values, better approximating the severity of the analyzed recessions. In contrast, global factors do not materially alter the densities relative to the reference model, confirming their limited additional predictive contribution.

Figure 7: Conditional densities and outturns for major crises

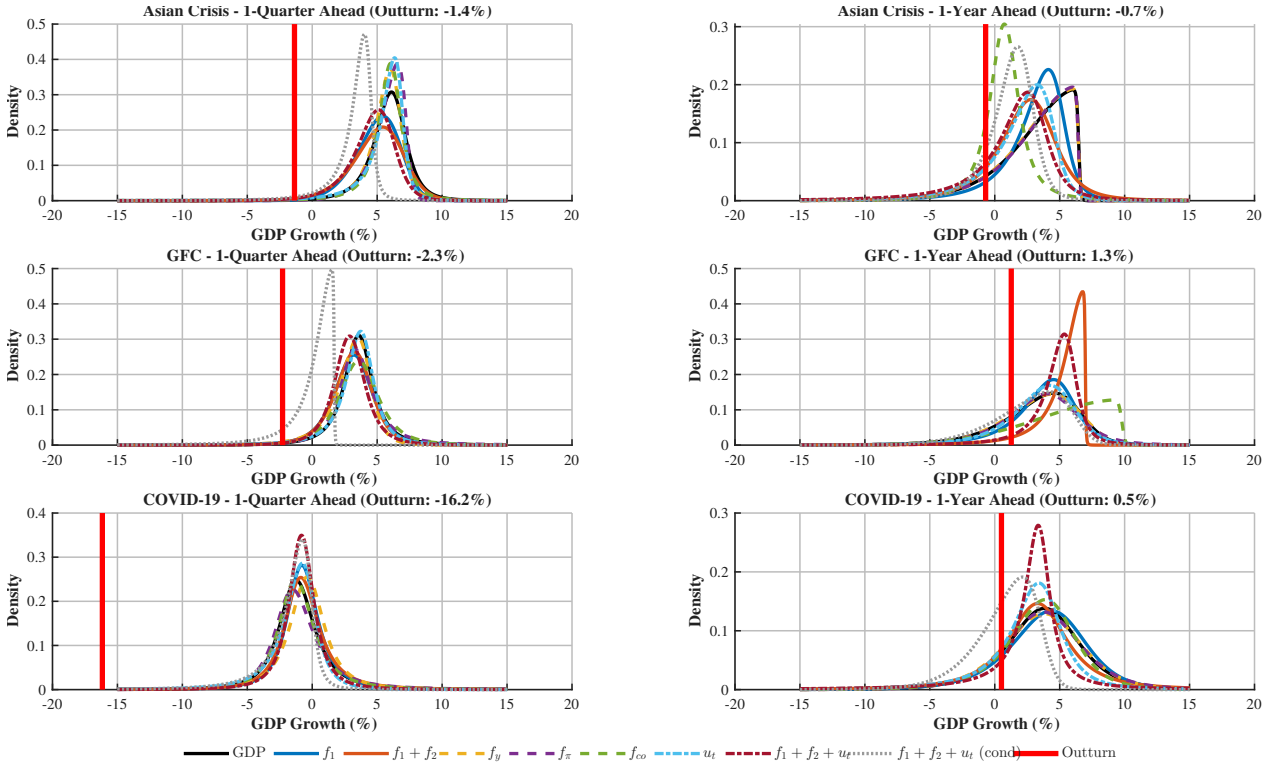

Notes: The panels in this figure show the estimated in-sample skewed t -density functions for one-quarter-ahead (left panel) and one-year- ahead (right panel) real GDP growth, along with the corresponding observed GDP growth outturns.

6.2 Growth-at-Risk (GaR)

Figure 8 depicts the evolution of the 5^{th} percentile of GDP growth at a one-year horizon, estimated in real time for each vintage as a measure of tail risk (GaR). Throughout the sample period, the 5^{th} percentile remains in negative territory—even during phases of relative stability—fluctuating between 0% and -5% across most specifications. This pattern reveals a persistent negative bias in the estimated distributions.

During stress episodes, declines are more pronounced. For instance, during the Covid-19 Pandemic, the conditional model incorporating unemployment rate leads anticipates a drop of approximately -6% in 2020Q2, whereas the observed outcome was -16.2%. In contrast, other specifications adjust only after the shock materializes, reacting with a lag both during the pandemic and the GFC. For example, the model with a single financial factor (blue line) predicts a 5^{th} percentile near -5% in 2009Q4 and -3% in 2021Q3, while the most severe contractions occurred in 2009Q2 (-2.9%) and 2020Q2 (-16.2%).

These results confirm that incorporating leading information substantially improves the ability to anticipate extreme risks, although it does not fully capture their magnitude. This performance surpasses that of traditional approaches based solely on contemporaneous information, which tend to reflect severe contractions only after they have occurred.

Figure 8: Estimated 5^{th} Percentile and GDP Growth Outturns (one-year-ahead)

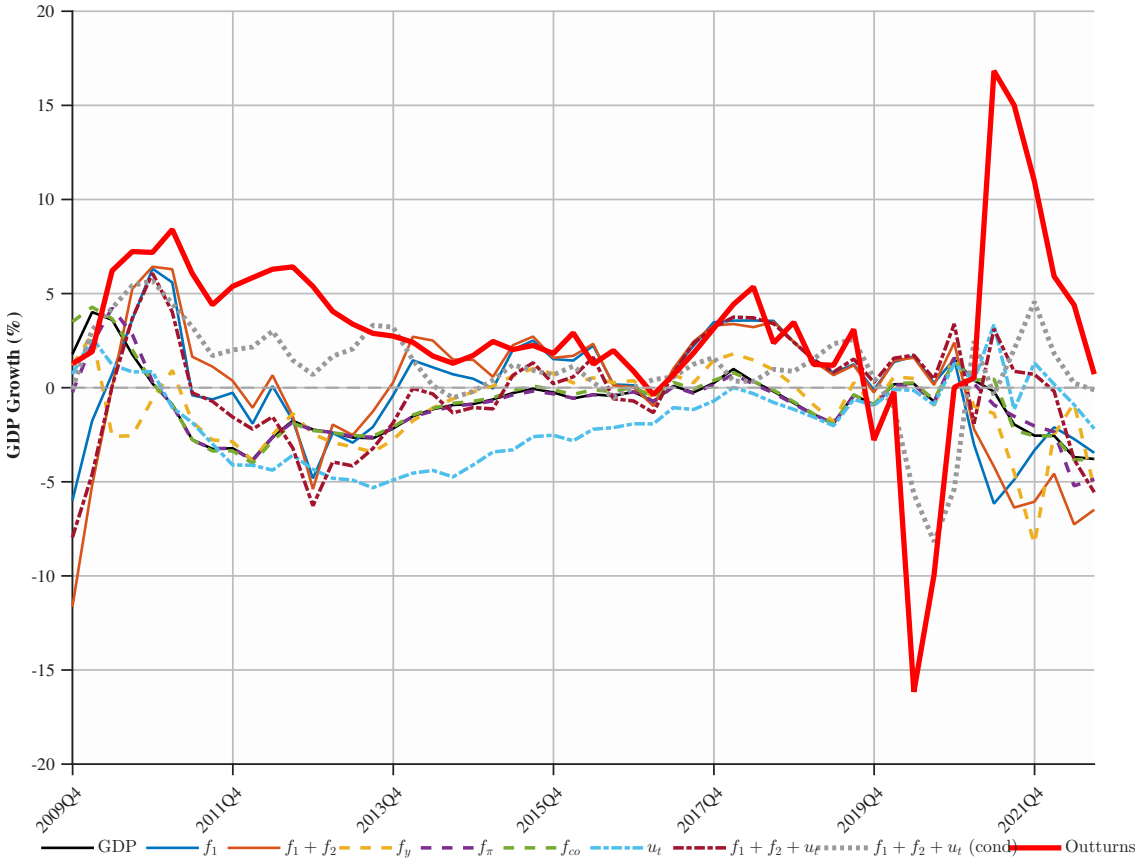

Notes: The chart plots the real-time estimates of the 5^{th} percentile of the predictive distribution for one-year-ahead real GDP growth, computed in real-time for each vintage from 2008Q4 to 2022Q3. Each point is the forecast at time t for growth at $t + 4$, based on information then available. The red line shows actual GDP growth. Lower values signal greater downside risk.

6.3 Probability of negative GDP Growth

Figure 9 shows the estimated real-time evolution of the probability that GDP growth will be negative at a one-year horizon. For most of the period, probabilities remain bounded at relatively low levels, around 10%, although some specifications reach values of about 20–30% during non-recession episodes, such as in 2012–2013, which is consistent with the negative bias previously observed in Growth-at-Risk measures. During the Covid-19 Pandemic, the conditional model that incorporates leads of the unemployment rate abruptly increases the probability of contraction, reaching levels close to 90% and anticipating the shock by one or two quarters, whereas the rest of the specifications react with a greater lag. A similar, though less

pronounced, pattern is observed around the GFC: the model with one domestic financial factor assigns a probability close to 35% in 2009Q4, despite actual growth being 1.3%.

Overall, leading labor market indicators markedly enhance early detection of contractions, whereas models relying only on contemporaneous data reveal vulnerabilities only after shocks occur.

Figure 9: Probability of negative GDP Growth (one-year ahead)

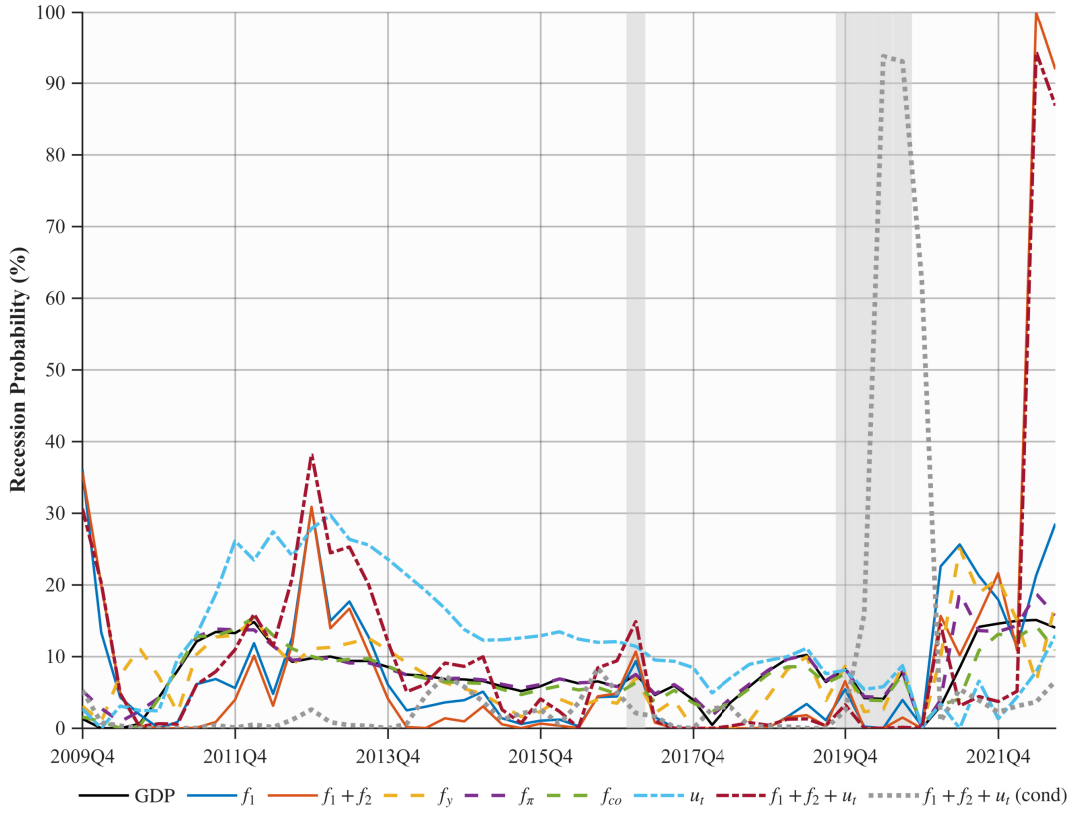

Notes: The chart shows the estimated probability of negative GDP growth at a one-year horizon (h=4), computed in real-time for each vintage from 2008Q4 to 2022Q3. Gray shading marks periods of actual negative GDP growth.

6.4 Fan charts

Figure 10 compares fan charts generated by the benchmark model—which conditions only on contemporaneous GDP growth—with those produced by the model incorporating financial factors and leading unemployment information, across two crisis episodes: the GFC and the Covid-19 Pandemic. During the GFC,

actual growth falls outside the benchmark model's fan chart in the first two quarters and in the lower part between the third and fifth quarters, whereas the conditional model includes it within the 70% interval up to the fourth quarter. Neither model succeeds in capturing the actual outcome from the fifth quarter onward. Moreover, the benchmark model's bands are relatively symmetric and wide, while the conditional model exhibits a more asymmetric distribution: it concentrates greater probability in the left tail during the contraction phase and shifts mass to the right during the recovery.

During the pandemic, both models include the actual outcome in the first three quarters but underestimate the subsequent recovery. However, the benchmark model contemplates more extreme scenarios in the initial phase—with bands reaching declines close to 20%—whereas the conditional model concentrates more mass around the actual outturn and assigns lower probability to extreme declines.

This evidence suggests that the proposed methodology enables the construction of conditional fan charts that offer a competitive alternative to traditional approaches. Its main advantages lie in capturing asymmetries inherent to the cycle and generating scenarios consistent with projected macro-financial conditions. This results in a more realistic representation of the balance of risks compared to methods based solely on historical forecast errors, which tend to produce symmetric bands and underestimate vulnerabilities during stress episodes.

Figure 10: GDP growth fan charts

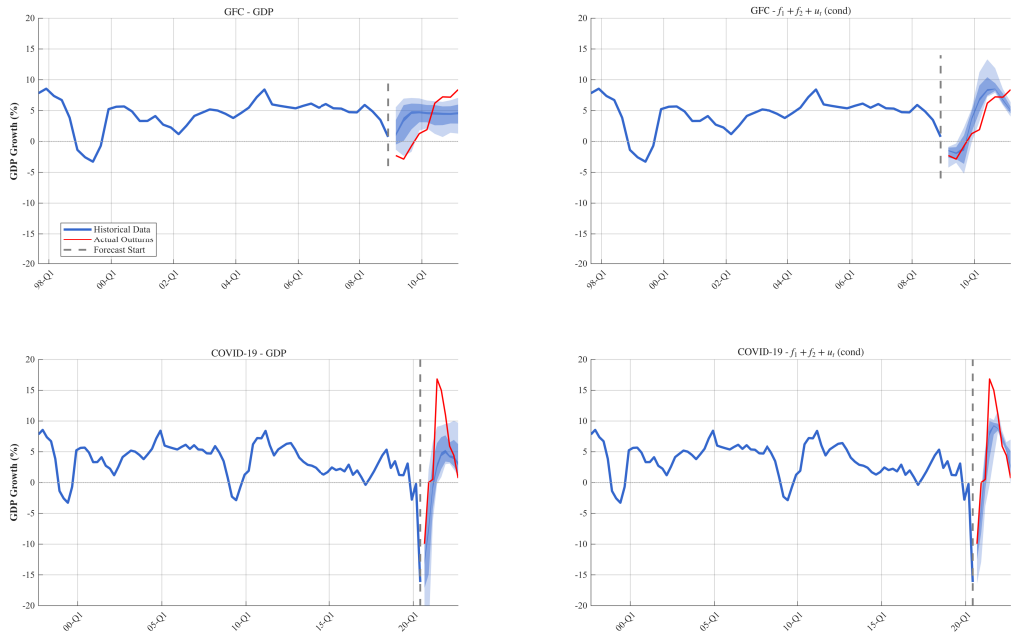

Notes: The figure presents fan charts comparing real-time GDP growth forecasts during two major crises: the GFC (2008Q4) and the Covid-19 Pandemic (2020Q2). Each panel displays the full predictive distribution for horizons 1 to 9 quarters ahead, with fan chart confidence intervals at 90%, 70%, and 10% levels constructed from fitted skewed-t distributions. The darker blue shading indicates regions of higher probability density. Historical GDP growth data available at the forecast origin is shown in blue, actual subsequent outturns in red, and the vertical dashed line marks the forecast cutoff. The left column shows forecasts from the baseline GDP model, while the right column presents results from the augmented model incorporating financial factors and unemployment rates. The forecasts are based on a CQR model estimated with data available as of the time of each forecast, and realized data for the technical assumptions over the projection horizon.

Overall, the applications demonstrate that the proposed methodology substantially enhances the ability to anticipate extreme risks and communicate scenarios under adverse conditions. Incorporating leading information—particularly unemployment rate leads—improves the allocation of probability to tail events and enables earlier identification of contraction episodes compared to approaches based exclusively on contemporaneous information. Likewise, the construction of conditional fan charts emerges as an effective tool for representing the balance of risks more realistically, capturing asymmetries and generating scenarios consistent with projected macro-financial conditions, thereby overcoming the limitations of methods based solely on historical forecast errors. Taken together, these findings underscore the value of the approach as an input for macro-financial monitoring and for communicating uncertainty in economic policy.

7 Robustness

To verify that the model rankings are not driven by the extreme volatility of the pandemic period, Table 2 reports relative GR scores for the pre-COVID evaluation window (2008Q4–2017Q3, 36 vintages), where the cutoff is chosen so that all forecast targets, including the longest horizon ($h = 9$), fall before 2020Q1. The core findings are preserved: the specification combining domestic financial factors with contemporaneous unemployment ($f_1 + f_2 + u_t$) consistently outperforms the benchmark across all horizons and regions of the distribution, with gains that strengthen at longer horizons—reaching a 29% reduction in unweighted GR scores at $h = 9$. The conditional specification with unemployment leads continues to dominate at short-to-medium horizons ($h \leq 6$), confirming that forward-looking labor-market information adds genuine predictive value beyond the pandemic episode. However, its advantage narrows at longer horizons ($h \geq 7$) and reverses in the tails at $h = 8$ and $h = 9$. This pattern is consistent with the interpretation advanced in Section 5: part of the conditional model's gains in the full sample reflects the strong contemporaneous linkage between unemployment and output during extreme episodes, rather than purely anticipatory content. In contrast, the specification with contemporaneous unemployment ($f_1+f_2+u_t$) delivers robust and horizon-stable improvements regardless of the sample period, reinforcing its suitability for operational forecasting.

Table 2: Relative Scores: Pre-COVID (2008Q4 – 2017Q3)

Model	h=1	h=2	h=3	h=4	h=5	h=6	h=7	h=8	h=9
Unweighted									
f_1	0.95	0.96	0.93	0.99	0.99	1.01	1.02	1.01	1.00
$f_1 + f_2$	0.97	1.00	0.93	0.92	0.93	**0.92**	0.92	0.99	1.02
f_y	1.04	1.00	0.99	1.00	1.00	0.95	0.98	1.00	1.00
f_π	1.01	0.97	0.99	0.99	1.03	1.09	1.05	1.02	1.02
f_{co}	1.00	1.02	1.00	0.97	0.93	0.90	0.91	0.96	0.98
u_t	1.00	1.01	1.12	1.04	0.93	0.93	0.91	0.86	**0.77**
$f_1 + f_2 + u_t$	0.96	0.90	0.87	0.84	0.85	0.87	0.83	0.81	**0.71**
$f_1 + f_2 + u_t$ (cond)	0.89	0.78	**0.75**	**0.75**	0.79	0.77	0.86	0.94	0.98
Centre									
f_1	0.95	0.95	0.91	0.98	0.99	1.02	1.02	**1.02**	1.01
$f_1 + f_2$	0.97	0.99	0.91	0.91	0.92	**0.91**	0.92	1.00	1.02
f_y	1.05	1.01	0.97	0.99	0.99	0.97	0.99	1.01	1.01
f_π	1.02	0.96	0.99	1.00	1.03	1.10	1.05	1.03	1.02
f_{co}	1.00	1.01	1.00	0.96	0.92	0.90	0.92	0.96	0.98
u_t	1.00	0.99	1.11	1.04	0.92	0.92	0.89	0.82	**0.74**
$f_1 + f_2 + u_t$	0.95	0.88	0.84	0.84	0.84	0.84	0.80	0.78	**0.68**
$f_1 + f_2 + u_t$ (cond)	0.90	0.78	**0.73**	**0.75**	0.76	0.76	0.83	0.91	0.93
Tails									
f_1	0.92	0.96	0.99	1.00	1.01	1.01	1.00	0.97	0.96
$f_1 + f_2$	0.99	1.03	1.01	0.97	0.95	**0.92**	0.91	0.95	1.02
f_y	1.01	0.99	1.07	1.01	1.01	0.90	0.91	0.96	0.99
f_π	0.98	0.99	0.99	0.97	1.00	1.05	1.03	1.01	1.02
f_{co}	1.00	1.03	1.03	1.02	0.95	0.90	0.89	0.97	0.99
u_t	1.01	**1.06**	**1.12**	1.04	0.94	0.99	1.00	1.00	0.91
$f_1 + f_2 + u_t$	0.97	0.95	0.97	0.86	0.86	0.98	0.96	0.94	0.82
$f_1 + f_2 + u_t$ (cond)	0.85	**0.76**	0.81	**0.74**	0.89	0.84	0.97	1.05	1.18
Right Tail									
f_1	0.96	0.96	0.91	0.94	0.98	1.00	1.02	1.00	1.00
$f_1 + f_2$	1.00	0.99	0.93	0.88	**0.86**	**0.91**	0.90	0.95	1.01
f_y	1.09	1.00	1.02	1.01	0.96	0.92	0.95	0.99	1.00
f_π	1.00	0.97	1.00	0.99	0.97	0.96	0.98	1.00	1.01
f_{co}	1.00	1.01	0.99	0.93	**0.88**	0.88	0.89	0.96	0.97
u_t	0.98	0.96	1.09	1.05	0.93	0.93	0.92	0.88	**0.82**
$f_1 + f_2 + u_t$	0.97	0.90	0.88	0.86	0.83	0.88	0.85	0.83	**0.77**
$f_1 + f_2 + u_t$ (cond)	0.86	0.76	0.78	**0.78**	0.77	0.80	0.80	0.87	0.90
Left Tail									
f_1	0.92	0.96	0.97	1.04	1.02	**1.03**	1.01	1.01	0.99
$f_1 + f_2$	0.95	1.02	0.96	0.98	1.00	**0.93**	0.93	1.02	1.04
f_y	0.98	1.01	0.98	0.99	1.04	0.97	0.98	1.00	1.00
f_π	1.01	0.97	0.98	0.99	1.07	1.22	1.11	1.05	1.03
f_{co}	1.00	1.03	1.03	1.03	0.99	0.92	0.93	0.96	0.99
u_t	1.03	**1.08**	1.15	1.04	0.93	0.96	0.93	0.88	0.77
$f_1 + f_2 + u_t$	0.94	0.91	0.89	0.83	0.87	0.90	0.85	0.84	**0.68**
$f_1 + f_2 + u_t$ (cond)	0.90	0.78	**0.74**	**0.72**	0.84	0.77	0.96	1.05	1.13

Notes: Relative GR scores, pre-COVID period 2008Q4–2017Q3 (36 vintages). An entry < 1 indicates that the augmented model outperforms the benchmark. The full-sample results (47 vintages) are reported in Table 1. Scores where the hypothesis of equal forecast accuracy is rejected at the 10% confidence level or higher based on the Diebold and Mariano (1995) test with the Harvey et al. (1997) finite-sample correction are highlighted in bold.

8 Conclusions

This paper proposes a Bayesian conditional quantile regression approach to estimate the full distribution of GDP growth in a small open economy. The method extends the Growth-at-Risk framework of Adrian et al. (2019) by incorporating expert judgment and future values of conditioning variables—particularly unemployment leads—into predictive densities, overcoming the limitation of models based solely on contemporaneous data.

Our contribution is twofold: (i) integrating domestic and global factors within a flexible Bayesian framework that accommodates lags and leads, improving estimation in small samples; and (ii) enhancing early detection of structural changes and downside risks by conditioning on leading labor market indicators, unlike previous frequentist approaches such as Alvarez et al. (2021).

The empirical application for Chile shows that domestic financial conditions and unemployment dynamics are key for assessing growth risks, while global factors add limited value. Including unemployment leads improves predictive performance across the distribution, reduces quantile loss, and enables timely identification of tail risks—whereas models without leading information react only after shocks like the GFC or Covid-19. Some forecasting gains reflect the counterfactual use of realized paths for the technical assumptions, yet strong performance under these conditions indicates the presence of economically meaningful relationships. In contrast, conditional forecasts that perform poorly even when conditioned on realized data lack practical relevance. Ultimately, while accuracy depends on the quality of assumed trajectories, the framework provides a coherent mapping from conditional information to predictive densities.

These findings are robust to the exclusion of the pandemic period from the evaluation sample, though the gains from the conditional specification narrow at long horizons in the pre-COVID subsample, consistent with the role of contemporaneous labor-market linkages during extreme episodes.

Finally, the framework supports conditional fan charts that reflect asymmetries and scenarios consistent with

conditioning paths, offering a robust tool for macro-financial monitoring and policy communication under uncertainty. Future work could extend this approach to multivariate systems integrating activity and inflation risks, strengthening central banks' capacity to map vulnerabilities.

References

Adrian, T., N. Boyarchenko, and D. Giannone (2019). Vulnerable Growth. *American Economic Reviw 109*(4), 1263–1289.

Alvarez, N., A. Fernandois, and A. Sagner (2021). Economic Growth at Risk: An Application to Chile. Working paper no. 905, Central Bank of Chile. Available at: https://www.bcentral.cl/en/content/-/details/working-papers-n-905.

Azzalini, A. and A. Capitanio (2003). Distributions Generated by Perturbation of Symmetry with Emphasis on a Multivariate Skew t-Distribution. *Journal of the Royal Statistical Society: Series B (Statistical Methodology) 65*(2), 367–89.

Birinci, S. and A. Amburgey (2021). How job separations differed between the great recession and covid-19 recession. Technical report, St Louis Fed.

Bjørnland, H. C., F. Ravazzolo, and L. A. Thorsrud (2017). Forecasting GDP with global components: This time is different. *International Journal of Forecasting 33*, 153–173.

Britton, E., P.G. Fisher, and J.D. Whitley (1998). The inflation report projections: understanding the fan chart. Bank of england quarterly bulletin: 30-37, Bank of England.

Charnavoki, V. and J. Dolado (2014). The Effects of Global Shocks on Small Commodity-Exporting Economies: Lessons from Canada. *American Economic Journal: Macroeconomics 6*(2), 207–37.

Diebold, F. X. and R. S. Mariano (1995). Comparing predictive accuracy. *Journal of Business & Economic Statistics 13*(3), 253–263.

Fornero, J. and A. Gatty (2020). Back testing fan charts of activity and inflation: the Chilean case. Working paper no. 881, Central Bank of Chile. Available at: https://www.bcentral.cl/documents/33528/133326/DTBC_881.pdf.

Gneiting, T. and R. Ranjan (2011). Comparing Density Forecasts Using Threshold- and Quantile-Weighted Scoring Rules. *Journal of Business and Economic Statistics 29*(3), 411–422.

Hamilton, J. D. (2011). Historical Oil Shocks. *National Bureau of Economic Research (NBER) Working Paper 16790*(16790), 52.

Harvey, D., S. Leybourne, and P. Newbold (1997). Testing the equality of prediction mean squared errors. *International Journal of Forecasting 13*(2), 281–291.

Khare, K. and J. P. Hobert (2012). Geometric ergodicity of the Gibbs sampler for Bayesian quantile regression. *Journal of Multivariate Analysis 112*, 108–116.

Kilian, L. (2006). Exogenous Oil Supply Shocks: How Big Are They and How Much Do They Matter for the U.S. Economy? *Review of Economics and Statistics 90*(2), 216–40.

Kilian, L. (2009). Not All Oil Price Shocks Are Alike: Disentangling Demand and Supply Shocks in the Crude Oil Market. *American Economic Review 99*(3), 1053–69.

Kilian, L. (2019). Measuring global real economic activity: Do recent critiques hold up to scrutiny? *Economics Letters 178*, 106–110.

Koenker, R. and B. G. Basset (1978). Regression Quantiles. *Econometrica 46*(1), 33–50.

Kohlbrecher, B. and C. Merkl (2022). Business cycle asymmetries and the labor market. *Journal of Macroeconomics 73*, 103458.

Kose, M. A., C. Otrok, and C. H. Whiteman (2003). International Business Cycles: World, Region, and Country-Specific Factors. *American Economic Review 93*(4), 1216–39.

Kozumi, H. and G. Kobayashi (2011). Gibbs sampling methods for Bayesian quantile regression. *Journal of Statistical Computation and Simulation 81*(11), 1565–1578.

Lyu, Y., J. Nie, and S.-K. Yang (2021). Forecasting US economic growth in downturns using cross-country data. *Economics Letters 198*(109668), 1–5.

McCracken, M. W. and J. T. McGillicuddy (2019). An empirical investigation of direct and iterated multistep conditional forecasts. *Journal of Applied Econometrics 34*(2), 181–204.

Miranda-Agrippino, S. and H. Rey (2020). U.S. Monetary Policy and the Global Financial Cycle. *Review of Economic Studies 87*(6), 2754–2776.

Mumtaz, H. and P. Surico (2009). The Transmission of International Shocks: A Factor-Augmented VAR Approach. *Journal of Money, Credit and Banking 41*(S1), 71–100.

Naudon, A. and A. Pérez (2018, April). Unemployment dynamics in chile: 1960-2015. *Journal Economía Chilena (The Chilean Economy) 21*(1), 004–033.

Ossandon, M., J. M. Sánchez-Martínez, A. Rodríguez-Martínez, R. Montañez-Enríquez, and S. Martínez-Jaramillo (2022). Growth at risk: Methodology and applications in an open-source platform. *Latin American Journal of Central Banking 3*(3), 1–21.

Plagborg-Møller, M., L. Reichlin, G. Ricco, and T. Hasenzagl (2020). When Is Growth at Risk? *Brookings Papers on Economic Activity 51*(1), 167–213.

Rossi, B. and T. Sekhposyan (2019). Alternative tests for correct specification of conditional predictive densities. *Journal of Econometrics 208*(2), 638–657.

Sokol, A. (2025). Fan charts 2.0: Flexible forecast distributions with expert judgement. *International Journal of Forecasting 41*(3), 1148–1164.

Yu, K. and R. A. Moyeed (2001). Bayesian quantile regression. *Statistics and Probability Letters 54*(4), 437–447.

A Appendix

Following Sokol (2025), let Y be a response variable and X a set of explanatory variables. Then, the linear regression model of Y is given by

$$y_t = x_t'\beta + \sigma\epsilon_t, \qquad t = 1, \ldots, T \tag{A.1}$$

where $\beta = \beta(q)$, the error term $\sigma\epsilon_t = \sigma(q)\epsilon_t(q)$ has a density function $f_q(\cdot)$ such that the q-th quantile equals zero, i.e. $\int_{-\infty}^{0} f_q(\sigma\epsilon_t)\, d\epsilon_t = q$, and $\sigma = \sigma(q) > 0$ is a scale parameter. For simplicity, let be $\sigma\epsilon_t = \varepsilon_t$.

The classical (frequentist) quantile regression estimation for β proceeds by minimizing

$$\sum_{t=1}^{T} \rho_q(y_t - x_t'\beta) \tag{A.2}$$

where $\rho_q(u) = u[q - I(u < 0)]$ is a check function and $I(\cdot)$ is an indicator function (see for example Koenker and Basset (1978)). Yu and Moyeed (2001) proposed a Bayesian modelling approach by noting that minimizing equation (A.2) is equivalent to maximizing a likelihood function under the asymmetric Laplace distribution for the error term with probability density function

$$f_q(\epsilon_t) = q(1-q)exp\{\rho_q(\epsilon_t)\} \tag{A.3}$$

with mean and variance given by

$$E(\epsilon_t) = \frac{1-2q}{q(1-q)}, \qquad Var(\epsilon_t) = \frac{1-2q+2q^2}{q^2(1-q)^2} \tag{A.4}$$

then, the error ε_t can be represented as a location-scale mixture of normals

$$\sigma\epsilon_t = \theta z_t + \tau\sqrt{\sigma z_t}u_t, \qquad t = 1, \ldots, T \tag{A.5}$$

where

$$\theta = \frac{1-2q}{q(1-q)}, \qquad \tau^2 = \frac{2}{q(1-q)} \tag{A.6}$$

Now, the quantile regression model becomes a normal linear regression model conditionally on z_t

$$y_t = x_t'\beta_q + \theta z_t + \tau\sqrt{\sigma z_t}u_t, \qquad t = 1, \ldots, T \tag{A.7}$$

where $z_t \sim \mathcal{E}(\sigma) = \sigma^{-1}\exp\left(-\sigma^{-1}z_t\right)$ and $u_t \sim \mathcal{N}(0,1)$ are mutually independent.

Key object for the Gibbs sampler: the joint density of $y = (y_1, \ldots, y_T)'$ given β_q, σ and $z = (z_1, \ldots, z_T)'$ is

$$\begin{aligned} f(y|\beta_q, z, \sigma) &= \prod_{t=1}^{T} f(y_t|\beta_q, z_t) = \prod_{t=1}^{T} \mathcal{N}(x_t'\beta_q + \theta z_t, \sigma\tau^2 z_t) && \text{(A.8)} \\ &= \prod_{t=1}^{T} \left(\frac{1}{\sqrt{2\sigma\tau^2 z_t}} \exp - \frac{(y_t - x_t'\beta_q - \theta z_t)^2}{2\sigma\tau^2 z_t} \right) && \text{(A.9)} \\ &= \propto \left(\prod_{t=1}^{T} \sigma^{-\frac{1}{2}} z_t^{-\frac{1}{2}} \right) \exp - \left\{ \sum_{t=1}^{T} \frac{(y_t - x_t'\beta_q - \theta z_t)^2}{2\sigma\tau^2 z_t} \right\} && \text{(A.10)} \end{aligned}$$

A.1 The Conditional Distribution

Following Azzalini and Capitanio (2003) in order to smooth the quantile function and recover a probability density function:

$$f(y; \mu, \sigma, \alpha, v) = \frac{2}{\sigma} t\left(\frac{y-\mu}{\sigma}; v\right) T\left(\alpha\frac{y-\mu}{\sigma}\sqrt{\frac{v+1}{v + \left(\frac{y-\mu}{\sigma}\right)^2}}; v+1\right), \tag{A.11}$$

$$\left\{\hat{\mu_{t+h}}, \hat{\sigma_{t+h}}, \hat{\alpha_{t+h}}, \hat{v_{t+h}}\right\} = \underset{\mu,\sigma,\alpha,v}{\arg\min} \sum_{\tau} \left(\hat{Q}_{t+h|x_t}(\tau|x_t) - F^{-1}(\tau;\mu,\sigma,v)\right)^2, \tag{A.12}$$

Assume

$\beta_q \sim \mathcal{N}(\beta_{q0}, B_{q0}), \qquad \sigma \sim \mathcal{IG}(\frac{\eta_0}{2}, \frac{s_0}{2})$

The full conditional density of β_q is a Gaussian distribution

$$\beta_q|y,z,\sigma \sim f(y|,\beta_q,z,\sigma)f(\beta_q)$$

$$= \left(\prod_{t=1}^{T} \mathcal{N}(x_t'\beta_q + \theta z_t, \sigma\tau^2 z_t)\right) \times \mathcal{N}(\beta_{q0}, B_{q0})$$

$$= \mathcal{N}(\hat{b_q}, \hat{B_q})$$

where

$$\hat{B_q^{-1}} = \sum_{t=1}^{T} \frac{x_t x_t'}{\sigma\tau^2 z_t} + B_{q0}^{-1}, \qquad \hat{\beta}_q = \hat{B}_q \left(\sum_{t=1}^{T} \frac{x_t(y_t - \theta z_t)}{\sigma\tau^2 z_t} + B_{q0}^{-1}\beta_{q0}\right)$$

The full conditional density of z_t is a generalized inverse Gaussian

$$z_t|\beta_q,z,y \sim f(y|\beta_q,z,\sigma)f(z)$$

$$= \left(\prod_{t=1}^{T} \mathcal{N}(x_t'\beta_q + \theta z_t, \sigma\tau^2 z_t)\right) \times \mathcal{E}(\sigma)$$

$$= \mathcal{GIG}(\frac{1}{2}, \hat{\delta}_t, \hat{\gamma}_t)$$

where

$$\hat{\delta}_t^2 = \frac{(y_t - x_t'\beta_q)^2}{\sigma\tau^2}, \qquad \hat{\gamma}_t = \frac{2}{\sigma} + \frac{\theta^2}{\sigma\tau^2}$$

The full conditional density of σ is a generalized inverse Gamma

$$\sigma|\beta_q, z, y \sim f(y|\beta_q, z, \sigma)f(\sigma)$$

$$= \left(\prod_{t=1}^{T} \mathcal{N}(x_t'\beta_q + \theta z_t, \sigma\tau^2 z_t)\right) \times \mathcal{IG}\left(\frac{\eta_0}{2}, \frac{s_0}{2}\right)$$

$$= \mathcal{IG}\left(\frac{\hat{\eta}}{2}, \frac{\hat{s}}{2}\right)$$

where

$$\hat{\eta} = \eta_0 + 3n, \qquad \hat{s} = s_0 + 2\sum_{t=1}^{T} z_t + \sum_{t=1}^{T} \frac{(y_t - x_t'\beta_q - \theta z_t)^2}{\tau^2 z_t}$$

B Data

Table B1: Domestic data sources and variable definitions

Variable	Short Name	Transformation	Source
EMBI Chile	EMBI		Central Bank of Chile (CBC)
IPSA Index	IPSA	Year-on-Year (YoY), NSA	CBC
IPSA volatility	σ		Bloomberg
Spread 30-90 days	SS		CBC
Corporate spread	SC		RiskAmerica
Yield of 10-years sovereign bond	BCP 10		CBC
Real Exchange Rate	RER	YoY	CBC
Terms of Trade	TOT	YoY	CBC
Industrial production index	IPI	YoY	CBC
Credit to GDP Gap	C/Y		Bank for International Settlements (BIS)
VIX	VIX		Federal Reserve Economic Data (FRED)

Table B2: External data sources and variable definitions

Variable	Short Name	Transformation	Source
Global Economic Activity			
Gross domestic product - OECD Total	GDP OECD	YoY	OECD
Gross domestic product - G7	GDP G7	YoY	OECD
Gross domestic product - EU15	GDP EU15	YoY	OECD
Gross domestic product – USA	GDP US	YoY	OECD
Industrial production - G7	IND G7	YoY	OECD
Industrial production - OECD Europa	IND EU15	YoY	OECD
Industrial production – USA	IND US	YoY	OECD
Export (Growth rate) - OECD Total	EXP OECD	YoY	OECD
Import (Growth rate) - OECD Total	IMP OECD	YoY	OECD
Index of Dry Cargo Bulk Freight Rates	DCBFR		Dallas Fed
Global Prices			
Price Deflators			
Deflator of gross domestic product - OECD Total	DGDP OECD	YoY	OECD
Deflator of gross domestic product - G7	DGDP G7	YoY	OECD
Deflator of gross domestic product - OECD Europa	DGDP EU	YoY	OECD
Deflator of gross domestic product - EU15	DGDP EU15	YoY	OECD
Deflator of gross domestic product – USA	DGDP US	YoY	OECD
Consumer price index, all items - OECD Total	CPI OECD	YoY	OECD
Consumer price index, all items - G7	CPI G7	YoY	OECD
Consumer price index, all items - OECD Europa	CPI EU	YoY	OECD
Consumer price index, all items - USA	CPI US	YoY	OECD
Consumer price index, non-food, non-energy - OECD Total	CPINEF OECD	YoY	OECD
Consumer price index, non-food, non-energy - G7	CPINEF G7	YoY	OECD
Consumer price index, non-food, non-energy - OECD Europa	CPINEF EU	YoY	OECD
Consumer price index, non-food, non-energy - USA	CPINEF US	YoY	OECD
Total producer prices, manufacturing - USA	PPIM US	YoY	OECD
Total producer prices, finished goods - USA	PPIFG US	YoY	OECD
World Commodity Prices			
Commodity price index, based on nominal US dollars, 2010=100 - Energy	RCP ENERGY	YoY	World Bank
Commodity price index, based on nominal US dollars, 2010=100 - Food	RCP FOOD	YoY	World Bank
Commodity price index, based on nominal US dollars, 2010=100 - Raw Materials	RCP RAW	YoY	World Bank
Commodity price index, based on nominal US dollars, 2010=100 - Base Metals	RCP METALS	YoY	World Bank
Commodity price index, based on nominal US dollars, 2010=100 - Fertilizers	RCP FERT	YoY	World Bank

Notes: Organization for Economic Cooperation & Development (OECD). YoY use non seasonally adjusted (NSA) data.

C Global and Domestic Factors

Figure C1: Estimated Factors

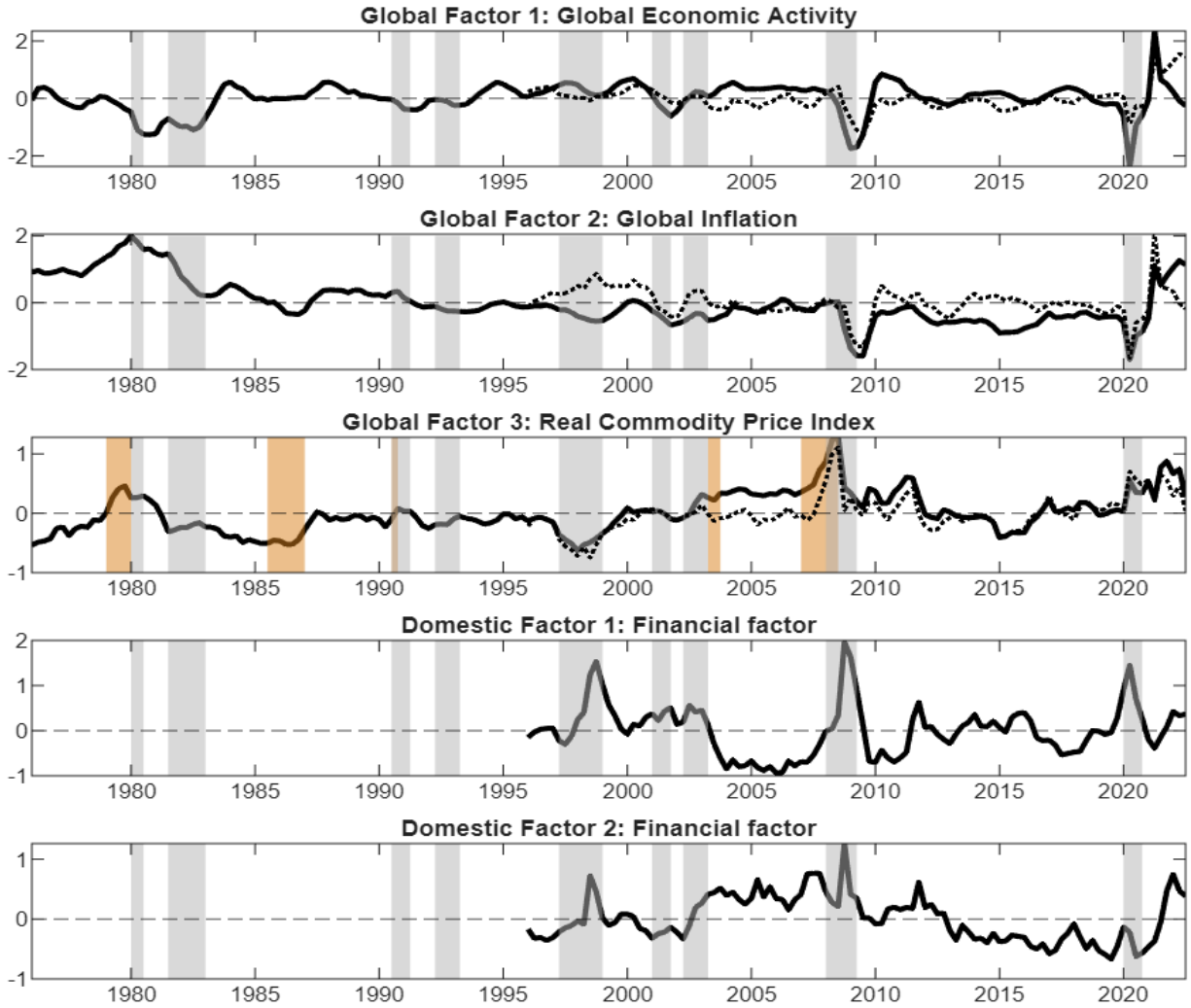

Notes: Gray (orange) shaded regions indicate major global recessions (key events in global commodity markets). Dotted lines represent orthogonalized global factors, obtained as residuals from regressing global factors on domestic factors.

Table C1: Relative Scores by Models and Horizons, Orthogonalized global factors

Model	h=1	h=2	h=3	h=4	h=5	h=6	h=7	h=8	h=9
Unweighted									
f_1	0.94	0.99	1.00	1.02	1.02	1.00	1.00	1.00	0.99
$f_1 + f_2$	0.95	1.00	0.98	0.93	**0.95**	**0.93**	0.95	1.00	1.01
f_y	1.00	1.03	1.06	1.03	0.98	0.99	1.01	1.01	1.00
f_π	1.00	1.00	1.06	1.08	1.04	0.99	0.99	1.00	1.00
f_{co}	1.00	1.02	**1.04**	**1.04**	1.00	0.98	0.98	1.01	1.01
u_t	1.00	0.99	1.02	0.99	0.93	**0.94**	0.95	0.94	0.92
$f_1 + f_2 + u_t$	0.94	0.94	0.94	0.88	**0.90**	**0.89**	0.91	0.92	0.89
$f_1 + f_2 + u_t$ (cond)	0.87	**0.71**	**0.69**	**0.70**	**0.71**	**0.69**	0.74	0.78	0.78
Centre									
f_1	0.94	0.99	0.98	1.01	1.02	1.01	1.00	1.00	1.00
$f_1 + f_2$	0.94	1.00	0.96	0.90	**0.93**	**0.92**	0.95	1.00	1.01
f_y	1.01	1.03	1.05	1.02	0.98	0.99	1.00	1.00	1.00
f_π	1.00	1.01	1.07	1.09	1.05	0.99	0.99	0.99	1.00
f_{co}	1.00	1.02	**1.04**	**1.04**	1.00	0.98	0.98	1.00	1.00
u_t	1.00	0.99	1.02	0.98	0.92	**0.92**	0.94	0.92	0.90
$f_1 + f_2 + u_t$	0.93	0.92	0.92	**0.85**	**0.88**	**0.86**	**0.89**	0.90	0.86
$f_1 + f_2 + u_t$ (cond)	0.87	**0.72**	**0.69**	**0.70**	**0.71**	**0.69**	**0.72**	0.77	0.76
Tails									
f_1	0.95	0.99	1.07	1.06	1.02	1.00	0.99	0.98	0.97
$f_1 + f_2$	0.97	1.02	1.05	1.00	0.99	**0.96**	0.97	1.00	1.00
f_y	0.99	1.04	1.10	1.04	0.98	1.00	1.02	1.02	1.00
f_π	1.00	0.98	1.04	1.08	1.02	0.99	1.00	1.01	1.00
f_{co}	1.00	1.03	1.04	**1.03**	1.00	0.98	0.99	1.04	1.01
u_t	1.00	1.00	1.00	1.00	0.95	0.98	1.01	1.01	1.00
$f_1 + f_2 + u_t$	0.96	1.01	1.03	0.95	0.97	0.97	0.99	1.01	0.97
$f_1 + f_2 + u_t$ (cond)	0.85	**0.68**	0.69	**0.70**	0.73	0.69	0.78	0.82	0.84
Right Tail									
f_1	0.95	0.98	0.96	0.98	1.00	1.00	1.00	1.01	1.00
$f_1 + f_2$	0.97	0.99	0.95	0.89	**0.90**	**0.94**	0.97	1.00	1.02
f_y	**0.99**	1.02	1.02	1.01	0.94	0.97	1.02	1.01	1.00
f_π	1.00	1.02	1.05	1.06	1.02	0.96	0.98	1.00	1.00
f_{co}	1.01	1.04	1.05	1.04	0.99	0.97	0.97	0.99	1.00
u_t	0.99	0.98	1.01	1.00	0.93	0.94	0.98	0.98	0.96
$f_1 + f_2 + u_t$	0.96	0.91	0.89	**0.85**	**0.88**	0.90	0.95	0.97	0.96
$f_1 + f_2 + u_t$ (cond)	0.88	**0.73**	**0.72**	**0.72**	**0.75**	**0.72**	**0.75**	0.80	0.80
Left Tail									
f_1	0.94	1.00	1.06	1.06	1.03	1.00	0.98	0.98	0.98
$f_1 + f_2$	0.94	1.02	1.02	0.99	1.00	**0.94**	**0.94**	0.99	1.00
f_y	1.00	1.04	1.10	1.05	1.01	1.02	1.01	1.01	1.00
f_π	1.00	0.98	1.07	1.11	1.06	1.02	1.00	1.00	1.00
f_{co}	1.00	1.01	**1.03**	**1.03**	1.01	0.99	1.00	1.04	1.02
u_t	1.01	1.00	1.02	0.98	0.93	0.94	0.95	0.93	0.92
$f_1 + f_2 + u_t$	0.93	0.99	1.01	0.93	0.95	0.91	**0.90**	0.91	0.86
$f_1 + f_2 + u_t$ (cond)	0.85	0.68	**0.66**	**0.68**	0.68	0.65	0.74	0.78	0.79

Notes: The table reports relative Gneiting and Ranjan (2011) scores over the forecast evaluation period 2008Q4 to 2022Q3, for a total of 47 vintages. The weight functions are given by $w_0 = 1$ (unweighted), $w_1(\tau) = \tau(1-\tau)$ (central region), $w_2(\tau) = (2\tau-1)^2$ (tails), $w_3(\tau) = \tau^2$ (right tail), and $w_4(\tau) = (1-\tau)^2$ (left tail). An entry < 1 indicates that the augmented model performs better than the model that conditions only in GDP in t in the region of interest. Orthogonalized global factors obtained as residuals from a regression of global factors against domestic factors. Scores where the hypothesis of equal forecast accuracy is rejected at the 10% confidence level or higher based on the Diebold and Mariano (1995) test with the Harvey et al. (1997) finite-sample correction are highlighted in bold.

Table C2: Relative Scores by Models and Horizons, Domestic factors and orthogonalized global factors

Model	h=1	h=2	h=3	h=4	h=5	h=6	h=7	h=8	h=9
Unweighted									
f_1	0.94	0.99	1.00	1.02	1.02	1.00	1.00	1.00	0.99
$f_1 + f_2$	0.95	1.00	0.98	0.93	**0.95**	**0.93**	0.95	1.00	1.01
$f_1 + f_2 + f_y$	1.00	1.03	0.97	0.93	0.97	0.95	0.95	0.99	1.01
$f_1 + f_2 + f_\pi$	0.96	1.02	1.01	0.95	0.98	0.96	0.96	0.99	1.02
$f_1 + f_2 + f_{co}$	0.95	1.02	0.99	0.96	0.96	0.95	**0.96**	0.98	1.01
$f_1 + f_2 + f_y + f_\pi + f_{co}$	1.00	1.04	1.01	1.00	1.04	1.09	0.99	0.99	1.04
$f_1 + f_2 + u_t$	0.94	0.94	0.94	0.88	**0.90**	**0.89**	0.91	0.92	0.89
$f_1 + f_2 + u_t(cond)$	0.87	**0.71**	**0.69**	**0.70**	**0.71**	**0.69**	0.74	0.78	0.78
Centre									
f_1	0.94	0.99	0.98	1.01	1.02	1.01	1.00	1.00	1.00
$f_1 + f_2$	0.94	1.00	0.96	0.90	**0.93**	**0.92**	0.95	1.00	1.01
$f_1 + f_2 + f_y$	1.00	1.03	0.95	0.91	0.96	0.94	0.94	0.98	1.01
$f_1 + f_2 + f_\pi$	0.95	1.01	1.00	0.94	0.98	0.95	0.95	0.99	1.02
$f_1 + f_2 + f_{co}$	0.95	1.01	0.97	0.94	0.94	0.94	**0.95**	0.97	1.01
$f_1 + f_2 + f_y + f_\pi + f_{co}$	1.00	1.04	0.99	0.98	1.03	1.07	0.98	0.98	1.04
$f_1 + f_2 + u_t$	0.93	0.92	0.92	**0.85**	**0.88**	**0.86**	**0.89**	0.90	0.86
$f_1 + f_2 + u_t(cond)$	0.87	**0.72**	**0.69**	**0.70**	**0.71**	**0.69**	**0.72**	0.77	0.76
Tails									
f_1	0.95	0.99	1.07	1.06	1.02	1.00	0.99	0.98	0.97
$f_1 + f_2$	0.97	1.02	1.05	1.00	0.99	**0.96**	0.97	1.00	1.00
$f_1 + f_2 + f_y$	1.00	1.06	1.05	1.01	1.02	1.00	0.97	1.00	1.00
$f_1 + f_2 + f_\pi$	0.97	1.02	1.05	0.97	1.01	0.99	0.97	0.99	1.01
$f_1 + f_2 + f_{co}$	0.98	1.05	1.08	1.02	1.00	0.99	0.98	1.01	1.01
$f_1 + f_2 + f_y + f_\pi + f_{co}$	0.99	1.06	1.08	1.06	1.07	1.13	1.01	1.03	1.07
$f_1 + f_2 + u_t$	0.96	1.01	1.03	0.95	0.97	0.97	0.99	1.01	0.97
$f_1 + f_2 + u_t(cond)$	0.85	**0.68**	0.69	**0.70**	0.73	0.69	0.78	0.82	0.84
Right Tail									
f_1	0.95	0.98	0.96	0.98	1.00	1.00	1.00	1.01	1.00
$f_1 + f_2$	0.97	0.99	0.95	0.89	**0.90**	**0.94**	0.97	1.00	1.02
$f_1 + f_2 + f_y$	1.03	1.01	0.94	0.89	**0.90**	0.92	0.96	1.00	1.01
$f_1 + f_2 + f_\pi$	0.97	1.00	1.03	0.94	0.94	0.92	0.96	0.99	1.01
$f_1 + f_2 + f_{co}$	0.98	1.00	0.97	0.95	**0.90**	**0.93**	0.96	0.97	1.00
$f_1 + f_2 + f_y + f_\pi + f_{co}$	1.03	1.01	1.01	0.99	0.95	0.99	0.96	0.97	1.02
$f_1 + f_2 + u_t$	0.96	0.91	0.89	**0.85**	**0.88**	0.90	0.95	0.97	0.96
$f_1 + f_2 + u_t(cond)$	0.88	**0.73**	**0.72**	**0.72**	**0.75**	**0.72**	**0.75**	0.80	0.80
Left Tail									
f_1	0.94	1.00	1.06	1.06	1.03	1.00	0.98	0.98	0.98
$f_1 + f_2$	0.94	1.02	1.02	0.99	1.00	**0.94**	**0.94**	0.99	1.00
$f_1 + f_2 + f_y$	0.97	1.06	1.02	0.99	1.05	1.00	0.94	0.98	1.00
$f_1 + f_2 + f_\pi$	0.95	1.03	1.01	0.97	1.03	1.00	0.96	0.99	1.01
$f_1 + f_2 + f_{co}$	0.94	1.04	1.04	0.99	1.02	0.99	**0.96**	1.00	1.01
$f_1 + f_2 + f_y + f_\pi + f_{co}$	0.97	1.07	1.03	1.03	1.13	1.19	1.02	1.03	1.08
$f_1 + f_2 + u_t$	0.93	0.99	1.01	0.93	0.95	0.91	**0.90**	0.91	0.86
$f_1 + f_2 + u_t(cond)$	0.85	0.68	**0.66**	**0.68**	0.68	0.65	0.74	0.78	0.79

Notes: The table reports relative Gneiting and Ranjan (2011) scores over the forecast evaluation period 2008Q4 to 2022Q3, for a total of 47 vintages. The weight functions are given by $w_0 = 1$ (unweighted), $w_1(\tau) = \tau(1-\tau)$ (central region), $w_2(\tau) = (2\tau-1)^2$ (tails), $w_3(\tau) = \tau^2$ (right tail), and $w_4(\tau) = (1-\tau)^2$ (left tail). An entry < 1 indicates that the augmented model performs better than the model that conditions only in GDP in t in the region of interest. Orthogonalized global factors obtained as residuals from a regression of global factors against domestic factors. Scores where the hypothesis of equal forecast accuracy is rejected at the 10% confidence level or higher based on the Diebold and Mariano (1995) test with the Harvey et al. (1997) finite-sample correction are highlighted in bold.

Table C3: Relative Scores: Pre-COVID (2008Q4 – 2017Q3)

Model	h=1	h=2	h=3	h=4	h=5	h=6	h=7	h=8	h=9
Unweighted									
f_1	0.95	0.96	0.93	0.99	0.99	1.01	1.02	1.01	1.00
$f_1 + f_2$	0.97	1.00	0.93	0.92	0.93	**0.92**	0.92	0.99	1.02
$f_1 + f_2 + f_y$	1.08	1.07	0.93	0.93	0.99	0.95	0.90	0.97	1.01
$f_1 + f_2 + f_\pi$	0.99	1.03	1.03	1.00	1.04	0.96	0.93	0.98	1.03
$f_1 + f_2 + f_{co}$	0.98	1.03	0.99	1.00	0.97	0.97	**0.92**	0.92	1.00
$f_1 + f_2 + f_y + f_\pi + f_{co}$	1.09	1.11	1.05	1.09	1.16	1.25	0.96	0.93	1.08
$f_1 + f_2 + u_t$	0.96	0.90	0.87	0.84	0.85	0.87	0.83	0.81	**0.71**
$f_1 + f_2 + u_t(cond)$	0.89	0.78	**0.75**	**0.75**	0.79	0.77	0.86	0.94	0.98
Centre									
f_1	0.95	0.95	0.91	0.98	0.99	1.02	1.02	**1.02**	1.01
$f_1 + f_2$	0.97	0.99	0.91	0.91	0.92	**0.91**	0.92	1.00	1.02
$f_1 + f_2 + f_y$	1.08	1.06	0.91	0.91	0.98	0.94	0.91	0.98	1.01
$f_1 + f_2 + f_\pi$	0.98	1.03	1.02	1.00	1.02	0.96	0.93	0.98	1.03
$f_1 + f_2 + f_{co}$	0.98	1.02	0.97	0.98	0.97	0.97	**0.92**	0.93	1.00
$f_1 + f_2 + f_y + f_\pi + f_{co}$	1.09	1.10	1.02	1.07	1.14	1.24	0.98	0.93	1.06
$f_1 + f_2 + u_t$	0.95	0.88	0.84	0.84	0.84	0.84	0.80	0.78	**0.68**
$f_1 + f_2 + u_t(cond)$	0.90	0.78	**0.73**	**0.75**	0.76	0.76	0.83	0.91	0.93
Tails									
f_1	0.92	0.96	0.99	1.00	1.01	1.01	1.00	0.97	0.96
$f_1 + f_2$	0.99	1.03	1.01	0.97	0.95	**0.92**	0.91	0.95	1.02
$f_1 + f_2 + f_y$	1.06	1.10	1.01	0.97	1.03	0.95	0.87	0.93	1.00
$f_1 + f_2 + f_\pi$	1.00	1.05	1.10	1.02	1.08	0.95	0.90	0.95	1.04
$f_1 + f_2 + f_{co}$	1.00	1.05	1.10	1.09	1.01	0.99	**0.90**	0.88	0.99
$f_1 + f_2 + f_y + f_\pi + f_{co}$	1.08	1.13	1.17	1.17	1.23	1.27	0.91	0.92	1.15
$f_1 + f_2 + u_t$	0.97	0.95	0.97	0.86	0.86	0.98	0.96	0.94	0.82
$f_1 + f_2 + u_t(cond)$	0.85	**0.76**	0.81	**0.74**	0.89	0.84	0.97	1.05	1.18
Right Tail									
f_1	0.96	0.96	0.91	0.94	0.98	1.00	1.02	1.00	1.00
$f_1 + f_2$	1.00	0.99	0.93	0.88	**0.86**	**0.91**	0.90	0.95	1.01
$f_1 + f_2 + f_y$	1.10	1.05	0.92	0.89	0.88	0.87	0.87	0.93	0.98
$f_1 + f_2 + f_\pi$	0.99	1.00	1.06	0.97	0.95	0.82	0.86	0.93	0.99
$f_1 + f_2 + f_{co}$	1.02	1.01	0.98	0.99	0.89	0.92	**0.89**	0.87	0.97
$f_1 + f_2 + f_y + f_\pi + f_{co}$	1.11	1.05	1.07	1.08	1.01	1.02	0.86	0.85	1.01
$f_1 + f_2 + u_t$	0.97	0.90	0.88	0.86	0.83	0.88	0.85	0.83	**0.77**
$f_1 + f_2 + u_t(cond)$	0.86	0.76	0.78	**0.78**	0.77	0.80	0.80	0.87	0.90
Left Tail									
f_1	0.92	0.96	0.97	1.04	1.02	**1.03**	1.01	1.01	0.99
$f_1 + f_2$	0.95	1.02	0.96	0.98	1.00	**0.93**	0.93	1.02	1.04
$f_1 + f_2 + f_y$	1.04	1.11	0.97	0.98	1.12	1.03	0.93	1.00	1.03
$f_1 + f_2 + f_\pi$	0.98	1.08	1.03	1.04	1.14	1.10	0.99	1.02	1.07
$f_1 + f_2 + f_{co}$	0.96	1.06	1.04	1.04	1.08	1.03	**0.93**	0.96	1.02
$f_1 + f_2 + f_y + f_\pi + f_{co}$	1.07	1.19	1.07	1.12	1.34	1.50	1.06	1.02	1.17
$f_1 + f_2 + u_t$	0.94	0.91	0.89	0.83	0.87	0.90	0.85	0.84	**0.68**
$f_1 + f_2 + u_t(cond)$	0.90	0.78	**0.74**	**0.72**	0.84	0.77	0.96	1.05	1.13

Notes: Relative GR scores, Pre-COVID (2008Q4 – 2017Q3) (36 vintages). An entry < 1 indicates that the augmented model outperforms the benchmark. The full-sample results are reported in Table C2. Orthogonalized global factors obtained as residuals from a regression of global factors against domestic factors. Scores where the hypothesis of equal forecast accuracy is rejected at the 10% confidence level or higher based on the Diebold and Mariano (1995) test with the Harvey et al. (1997) finite-sample correction are highlighted in bold.

Documentos de Trabajo Banco Central de Chile	Working Papers Central Bank of Chile
NÚMEROS ANTERIORES	PAST ISSUES
La serie de Documentos de Trabajo en versión PDF puede obtenerse gratis en la dirección electrónica: www.bcentral.cl/esp/estpub/estudios/dtbc. Existe la posibilidad de solicitar una copia impresa con un costo de Ch$500 si es dentro de Chile y US$12 si es fuera de Chile. Las solicitudes se pueden hacer por fax: +56 2 26702231 o a través del correo electrónico: bcch@bcentral.cl.	Working Papers in PDF format can be downloaded free of charge from: www.bcentral.cl/eng/stdpub/studies/workingpaper. Printed versions can be ordered individually for US$12 per copy (for order inside Chile the charge is Ch$500.) Orders can be placed by fax: +56 2 26702231 or by email: bcch@bcentral.cl.

DTBC – 1081
Conditional Bayesian Quantile Regressions for Forecasting the GDP Growth Distribution in a Small Open Economy
Jorge Fornero, Carlos Molina

DTBC – 1080
Fundamental Drivers of Financial Conditions
Elías Albagli, Guillermo Carlomagno, Javier Ledezma, María Teresa Reszczynski

DTBC – 1079
Hospital Choice, C-sections, and long-term maternal health
Ramiro de Elejalde, Eugenio Giolito

DTBC – 1078
Zero Energy Day: How Nationwide Blackouts Affect the Economy
Luis Gonzales, Koichiro Ito, Mar Reguant

DTBC – 1015 (Updated)
Fiscal Consolidations in Commodity-Exporting Countries: A DSGE Perspective
Manuel González-Astudillo , Juan Guerra-Salas , Avi Lipton

DTBC – 1077
Un sistema de proyección de demanda por efectivo en Chile: Actualización y propuesta
Nicolás Leiva, Carlos A. Medel

DTBC – 1076
Inflation Heterogeneity and Differential Effects of Monetary and Oil Price Shocks
Felipe Martínez

DTBC – 1075
Consumption Insurance over the Life Cycle
Enzo Cerletti, Tomás Cortés

DTBC – 1074
Precios de viviendas en Chile: Herramientas para Evaluar Desalineamientos y sus Efectos sobre la Banca
Serio Díaz V., Mauricio Salas G., Francisco Vásquez L.

DTBC – 1073
The Life Experience of Central Bankers and Monetary Policy Decisions: A Cross-country Dataset
Carlos Madeira

DTBC – 1072
Coordinating in the Haircut. A Model of Sovereign Debt Restructuring in Secondary Markets
Adriana Cobas

DTBC – 1070
Climate Transition Risks in Chile's Banking Industry: A Loan-Level Stress Test
Felipe Córdova, Francisco Pinto, Mauricio Salas

DTBC – 1069
How accurately do consumers report their debts in household surveys?
Carlos Madeira

DTBC – 1068
Riesgo de Crédito Gestionado por Medio de un Modelo de Espacio-Estado Aplicado a un Portafolio Soberano
Pablo Tapia, Diego Vargas

DTBC – 1067
Macroeconomic Effects of Carbon-intensive Energy Price Changes: A Model Comparison Matthias Burgert, Matthieu Darracq Pariès, Luigi Durand, Mario González, Romanos Priftis, Oke Röhe, Matthias Rottner, Edgar Silgado-Gómez, Nikolai Stähler, Janos Varga

DTBC - 1066
Bank Branches and the Allocation of Capital across Cities
Olivia Bordeu, Gustavo González, Marcos Sorá

DTBC – 1065
Effects of Tariffs on Chilean Exports
Lucas Bertinatto, Lissette Briones, Jorge Fornero

DOCUMENTOS DE TRABAJO Mayo 2026